Bacteria Are a Major Determinant of Orsay Virus Transmission and Infection in *Caenorhabditis elegans*

Brian G. Vassallo[1,2], Noémie Scheidel[1], Sylvia E. J. Fischer[1], and Dennis H. Kim[1,*]

1. Division of Infectious Diseases, Department of Pediatrics, Boston Children's Hospital and Harvard Medical School; Boston, 02115, USA
2. Department of Biology, Massachusetts Institute of Technology; Cambridge, 02139, USA

*Corresponding author. Email: dennis.kim@childrens.harvard.edu

Abstract

The microbiota is a key determinant of the physiology and immunity of animal hosts. The factors governing the transmissibility of viruses between susceptible hosts are incompletely understood. Bacteria serve as food for *Caenorhabditis elegans* and represent an integral part of the natural environment of *C. elegans.* We determined the effects of bacteria isolated with *C. elegans* from its natural environment on the transmission of Orsay virus in *C. elegans* using quantitative virus transmission and host susceptibility assays. We observed that *Ochrobactrum* species promoted Orsay virus transmission, whereas *Pseudomonas lurida* MYb11 attenuated virus transmission relative to the standard laboratory bacterial food *Escherichia coli* OP50. We found that pathogenic *Pseudomonas aeruginosa* strains PA01 and PA14 further attenuated virus transmission. We determined that the amount of Orsay virus required to infect 50% of a *C. elegans* population on *P. lurida* MYb11 compared with *Ochrobactrum vermis* MYb71 was dramatically increased, over three orders of magnitude. Host susceptibility was attenuated even further in presence of *P. aeruginosa* PA14. Genetic analysis of the determinants of *P. aeruginosa* required for attenuation of *C. elegans* susceptibility to Orsay virus infection revealed a role for regulators of quorum sensing. Our data suggest that distinct constituents of the *C. elegans* microbiota and potential pathogens can have widely divergent effects on Orsay virus transmission, such that associated bacteria can effectively determine host susceptibility versus resistance to viral infection. Our study provides quantitative evidence for a critical role for tripartite host-virus-bacteria interactions in determining the transmissibility of viruses among susceptible hosts.

37 **Introduction**

38 Viruses are ubiquitous and abundant[1,2]. Infection can have profound consequences for
39 the health of an individual host. The ability of viruses to transmit from one individual to another
40 can scale these consequences causing morbidity and mortality throughout whole populations.
41 Many factors influence virus transmission[3–5]. Abiotic factors such as temperature[6] and humidity[7]
42 and biotic factors such as viral load[8,9] and host immune status[10,11] all interact to determine
43 transmission rates. Despite these findings, the determinants of virus transmissibility remain
44 incompletely understood.

45 The microbiota has emerged as a host-associated factor that modulates multiple aspects
46 of virus infection and thereby alters transmission rates among host organisms[12–14]. In general,
47 the microbiota is critical for the proper development of the immune system and for the effective
48 activation of antimicrobial immune responses even at sites distal to microbiota colonization[15].
49 More specifically, bacteria and bacterial surface structures such as lipopolysaccharide and
50 peptidoglycan have been shown to stabilize poliovirus and reovirus *in vitro*[13,16]. These
51 observations likely explain why microbiota depletion by antibiotic treatment was sufficient to
52 provide protection against the same viruses in mice[13]. The bacterial symbiont *Wolbachia* protects
53 numerous insect species from multiple viruses either by upregulating antiviral defenses or
54 competing for intracellular nutrients[17–21]. Individual bacteria have also been found to enhance
55 viral infection; *Serratia marcescens* promoted infection of the mosquito *Aedes aegypti* by
56 Dengue, Zika, and Sindbis viruses by secreting a protein, enhancin, that degrades the mucus layer
57 covering epithelial cells[14].

58 *Caenorhabditis elegans* is a nematode often found in microbially rich environments such
59 as rotting vegetation[22]. The first naturally occurring virus capable of infecting the *C. elegans* was
60 isolated from Orsay, France[23]. Orsay virus is a part of a group of nematode infecting viruses
61 closely related to the *Nodaviridae* family of viruses which infect arthropods and fish[23,24]. Like
62 other Nodaviruses, Orsay virus is a positive-sense, single-stranded RNA virus with a bipartite
63 genome[23]. Transmission of Orsay virus occurs horizontally through the fecal-oral route.
64 Fluorescence *in situ* hybridization and immunofluorescence imaging has revealed that Orsay virus
65 solely infects *C. elegans* intestinal cells[23,25]. Viral infection activates host defense mechanisms
66 including the RNA-interference response and a transcriptional program known as the
67 intracellular pathogen response[23,26–29].

68 *C. elegans* is a bacterivore and is propagated in the laboratory on lawns of *Escherichia coli*
69 OP50. *Pseudomonas aeruginosa,* an opportunistic pathogen of humans, is found in the soil and
70 water and can also infect *C. elegans*[30–32]. Infection of *C. elegans* with *P. aeruginosa* activates
71 innate immunity and stress responses, as well as behavioral avoidance responses[33–35]. Recently,
72 the bacteria resident in the natural environment of *C. elegans* in the wild have been of increasing
73 interest[22,36–38]. The intestinal lumen of free-dwelling *C. elegans* is occupied by taxonomically and
74 functionally diverse bacteria that can affect *C. elegans* fitness and physiology[36,37,39].

75 In this study, we sought to understand how bacteria that are constituents of the *C.*
76 *elegans* microbiota quantitatively affect the transmission of Orsay virus in *C. elegans.* We
77 observed that monoaxenic cultures of different bacterial species had widely divergent effects on
78 the transmission of Orsay virus and conducted genetic analysis of the bacterial determinants

79 involved in modulating virus transmission. Our data point to a key species-specific role for
80 bacteria as critical determinant of virus transmission.
81
82 **Results**
83 **Wide variation in the effects of bacteria on the transmission of Orsay virus.**
84 Orsay virus spreads horizontally through the fecal-oral route and transmission can spread
85 from a single animal to a population of animals on a plate[40]. We sought to assess the impact of
86 bacteria on Orsay virus transmission rates and utilized a collection of bacteria isolated from the
87 environment with wild *C. elegans* to assemble a panel of Gram-negative bacteria for comparison
88 with the standard laboratory bacterial food, *Escherichia coli* OP50[36,37,39,41,42]. All animals were
89 raised to young adulthood on lawns of *E. coli* OP50 to eliminate differences in developmental
90 rates caused by different bacteria[39]. We set up a transmission assay by placing infected animals
91 ("spreaders") together with uninfected animals on a monoaxenic lawn of each test bacterium.
92 We quantified the incidence proportion, defined as the number of new infections produced after
93 24 h as determined by detection of induction of the *pals-5p::GFP* reporter, which is induced by
94 infection with Orsay virus (Fig. 1A-C)[27]. We observed a wide range in the measured incidence
95 proportion (Fig. 1B and 1C). Exposure to many of the naturally associated bacterial strains
96 resulted in transmission that was comparable to the incidence proportion observed with *E. coli*
97 OP50 with some prominent exceptions (Fig. 1B and 1C). Two *Ochrobactrum* species promoted
98 virus infection in nearly all individuals in the transmission assay and increased the incidence
99 proportion 2.7-fold and 2.9-fold compared to *E. coli* OP50 (Fig. 1B and 1C). We confirmed that
100 transmission from the initial spreader animals in the assay, and not multiple rounds of infection,
101 was responsible for the increased incidence proportion observed in the presence of

102 *Ochrobactrum vermis* MYb71 (Supp. Fig. 1A-D). On the other hand, the presence of *P. lurida*
103 MYb11 reduced the incidence proportion 4.1-fold compared to *E. coli* OP50 and 11-fold
104 compared to *O. vermis* MYb71 (Fig. 1B and C). These results present a striking divergence in the
105 effects of individual bacterial constituents of the *C. elegans* microbiota on the level of
106 transmission of Orsay virus from infected animals.

107 We reasoned that increased transmission of Orsay virus could be due to bacterial
108 modulation of host susceptibility to viral infection. To quantify the degree of host susceptibility
109 to Orsay virus we added Orsay virus in doses that ranged across four orders of magnitude and
110 then measured the fraction of individuals that became *pals-5p::GFP* positive after 24 h (Fig. 1A
111 and 1D, Supp. Fig. 2 and Supp. Fig. 3). We also specifically calculated the ID_{50}, or the dose of Orsay
112 virus required to infect 50% of the population after 24 h of exposure (Fig. 1D and 1E, Supp. Fig
113 2). On average, 3.6 μL of Orsay virus stock prepared as indicated in the Methods was required to
114 infect 50% of a population of ZD2611 animals in the presence of *E. coli* OP50 after 24 hours (Supp.
115 Fig. 2). We observed variability in the measured ID_{50} even when using the same batch of Orsay
116 virus (e.g. Fig. 1D vs Supp. Fig. 3A vs. Supp. Fig. 3B). We therefore chose to control all our
117 experiments internally rather than attempt to normalize between Orsay virus batches and we
118 report doses used in arbitrary units (a.u.), however 1 a.u. corresponds to 1 μL of Orsay virus
119 filtrate (Methods).

120 To determine quantitatively how different bacterial species modulate host susceptibility
121 to viral infection independently of the potential differential effects of bacteria on host shedding
122 of viruses, we added fixed doses of Orsay virus to plates of each bacterial species and monitored
123 infection using the *pals-5p::GFP* reporter. At lower doses of Orsay virus, the presence of *O. vermis*

124 MYb71 resulted in a higher fraction of infected animals than those observed in the presence of
125 *E. coli* OP50 or *P. lurida* MYb11 (Fig. 1D, Supp. Fig. 3). At higher doses of Orsay virus, the presence
126 of *P. lurida* MYb11 resulted in a reduced fraction of infected animals compared to *O. vermis*
127 MYb71 and *E. coli* OP50 (Fig. 1D, Supp. Fig 3). We further quantified the ID_{50} in the presence of
128 each bacterium and on average we observed that the ID_{50} in the presence of *E. coli OP50* was 14-
129 fold higher than the ID_{50} in the presence of *O. vermis* MYb71 (Fig. 1D and 1E, Supp. Fig. 3). The
130 ID_{50} observed in the presence of *P. lurida* was 120-fold and 1800-fold higher than the ID_{50} in the
131 presence of *E. coli* OP50 or *O. vermis* MYb71 respectively (Fig. 1D and 1E, Supp. Fig. 3).

132 We corroborated our observations from the *pals-5p::GFP* reporter by scoring the same
133 samples using fluorescence *in situ* hybridization to detect the RNA1 segment of the Orsay virus
134 genome in the intestinal cells of infected animals (Fig. 1F). As expected, we observed that at lower
135 doses the presence of *O. vermis* MYb71 resulted in a greater fraction of infected animals
136 compared to *E. coli* OP50 or *P. lurida* MYb11, while at higher doses the presence of *P. lurida*
137 MYb11 resulted in a reduced fraction of infected animals (Fig. 1F). Together these data establish
138 that individual members of the *C. elegans* microbiota can modulate host susceptibility to Orsay
139 virus over three orders of magnitude with dramatic consequences for the transmissibility of
140 Orsay virus.

141 We also assessed whether bacteria altered host feeding behavior as this may influence
142 the transmission and infection rate of Orsay virus. We quantified the number of pharyngeal
143 pumps per minute (ppm), a metric of *C. elegans* feeding, in the presence of each bacterium. After
144 6 h of exposure to *E. coli* OP50, *P. lurida* MYb11, or *O. vermis* MYb71 there were no differences
145 in pharyngeal pumping rates (Supp. Fig. 4A). At 24 h pumping rates were decreased in the

146 presence of *O. vermis* MYb71 to an average of 242 ppm compared to 261 ppm in the presence
147 of *P. lurida* MYb11 suggesting that changes to feeding behavior are unlikely to be responsible for
148 observed effects on host susceptibility to Orsay virus (Supp. Fig. 4B).
149

150 ***P. aeruginosa* attenuates Orsay virus transmission.**

151 In view of the effect of *P. lurida* MYb11 on attenuating Orsay virus infection of *C. elegans,*
152 we examined the effect of the distantly related bacterium, *Pseudomonas aeruginosa,* an
153 opportunistic pathogen of humans that has been characterized extensively[30,43]. We observed
154 that in the presence of either *P. aeruginosa* strains PA01 or PA14, transmission from spreader
155 animals to uninfected individuals was nearly completely blocked and the incidence proportion
156 was 11-fold and 32-fold lower than that observed in the presence of *E. coli* OP50, respectively
157 (Fig. 2A). The attenuating effect of *P. aeruginosa* PA01 and PA14 on virus transmission was
158 further reduced 3.1-fold and 9.5-fold, respectively, compared to the incidence proportion
159 observed in the presence of *P. lurida* MYb11 (Fig. 2A).

160 We confirmed that host susceptibility to Orsay virus was reduced in the presence of *P.*
161 *aeruginosa* by performing susceptibility assays at two doses of exogenous Orsay virus (Fig 2B,
162 Supp. Fig. 5). At each dose, fewer animals were infected following exposure to equivalent doses
163 of Orsay virus in the presence of *P. aeruginosa* PA01, PA14, or *P. lurida* MYb11 as compared to
164 the fraction of animals infected in the presence of *E. coli* OP50 (Fig. 2B, Supp. Fig. 5). At the
165 highest dose of virus used, we still observed robust attenuation of infection in the presence of *P.*
166 *aeruginosa* PA14 as 0.5% of the animals were infected as compared to 54%, 70%, and 97% in the
167 presence of *P. aeruginosa* PA01, *P. lurida* MYb11, or *E. coli* OP50, respectively (Fig. 2B). We

168 confirmed that no individuals were detectably infected with Orsay virus while in the presence of
169 *P. aeruginosa* PA14 using FISH staining (Fig. 2C). FISH additionally confirmed that the presence of
170 *P. aeruginosa* PA01 and *P. lurida* MYb11 attenuated average infection to 24% and 60% of the
171 population respectively compared to *E. coli* OP50 which supported infection of 86% of the
172 population. Further, *P. aeruginosa* PA01, *P. lurida* MYb11, and *E. coli* OP50 all supported higher
173 levels of infection than *P. aeruginosa* PA14. (Fig. 2C). Together these results demonstrate a
174 striking capacity of *P. lurida* MYb11 and *P. aeruginosa* strains to sharply reduce and even
175 effectively block, host susceptibility to infection with Orsay virus.

176 We again assessed whether bacterial modulation of host feeding behavior may be
177 responsible for the observed effects on host susceptibility to Orsay virus. There were no
178 differences observed in pharyngeal pumping rate after 6 h of exposure to each bacterium (Supp.
179 Fig. 4A). After 24 h pharyngeal pumping rate increased in the presence of *P. aeruginosa* PA14 to
180 an average of 264 ppm compared to 248 ppm in the presence of *E. coli* OP50 which suggests that
181 changes to feeding behavior are unlikely to account for the attenuation of infection observed in
182 *P. aeruginosa* (Supp. Fig. 4B).

183 *P. aeruginosa* is a pathogen of *C. elegans* and numerous other organisms[30,44,45].
184 Moreover, while both PA01 and PA14 are pathogenic, PA14 is more virulent towards *C. elegans*[30].
185 *P. lurida* MYb11 promotes developmental rate and fitness, although does so at a minor cost to
186 overall lifespan[39,46]. The effect of O. vermis MYb71 on lifespan has not been assessed. We
187 assessed host lifespan under our assay conditions to examine links between bacterial
188 pathogenicity and host susceptibility to Orsay virus. Under our assay conditions, including a full
189 lawn of bacteria, which prevent *C. elegans* from avoiding undesirable bacteria, and a temperature

190 of 20°C, which is below the optimal virulence temperature of *P. aeruginosa,* substantial mortality
191 is not observed until 72 hours after exposure (Supp. Fig. 6). All bacteria enhanced mortality in
192 comparison to *E. coli* OP50 (Supp. Fig. 6). Interestingly, *O. vermis* MYb71 exposure led to similarly
193 enhanced mortality when compared to *P. aeruginosa* PA14, and both bacteria enhanced
194 mortality in comparison to *P. lurida* MYb11 or *P. aeruginosa* PA01 (Supp. Fig. 6). *P. lurida* MYb11
195 also enhanced mortality compared to *P. aeruginosa* PA01 under these conditions (Supp. Fig. 6).
196 The similar lifespans of animals exposed to *P. aeruginosa* PA14 and *O. vermis* MYb71 stand in
197 contrast to their divergent effects on host susceptibility to Orsay virus. This suggests that general
198 pathogenicity is unlikely to be responsible for effects on host susceptibility, although pathogenic
199 consequences specific to exposure to each bacterium may still contribute to the observed effects
200 on host susceptibility to Orsay virus.
201

202 **Attenuation of Orsay virus transmission by *P. lurida* and *P. aeruginosa* is not due to effects on**
203 **Orsay virus replication, stability, or shedding.**

204 We considered the possibility that the attenuation of Orsay virus transmission in the
205 presence of *P. lurida* and *P. aeruginosa* strains might be due to inhibitory effects of the bacteria
206 on the replication of Orsay virus once transmitted to a susceptible animal host. To evaluate this
207 possibility, we made use of a plasmid-based system in which viral RNA1 is expressed through a
208 transgene introduced into *C. elegans,* so that replication of RNA1 can be assessed independent
209 of the entry of exogenous virus into the host[47]. In this system, the Orsay virus RNA1 segment,
210 which encodes the RNA-dependent RNA polymerase (RdRP), is expressed following heat-shock.
211 The expressed RNA1 may then be translated to produce the RdRP which can then replicate RNA1
212 through a negative-strand intermediate. The expression of RNA1 via heat-shock bypasses any

213 differences in viral entry or pre-replication steps, allowing for a direct test of RNA1 replication
214 efficiency under different conditions[47]. A plasmid expressing a mutated RdRP (RNA1[D601A])
215 incapable of supporting further RNA1 replication after the initial heat-shock serves as a control
216 for heat shock efficiency[47]. Using this system, we observed that Orsay virus RNA1 replication
217 efficiency was unaffected by the presence of *Pseudomonas* species relative to RNA1 replication
218 observed in the presence of *E. coli* OP50 (Fig. 3A). Additionally, there were no differences
219 observed in heat-shock efficiency between the different bacteria (Fig. 3A). These data suggest
220 that bacteria-induced differences in RNA1 replication in the host do not explain the substantial
221 attenuation of Orsay virus transmission and infection rates caused by *P. aeruginosa* PA01 or PA14
222 and *P. lurida* MYb11.

223 We sought to confirm the successful replication of the plasmid expressed RNA1 of Orsay
224 virus by assessing whether we could detect the replication of Orsay virus RNA1 in each
225 *Pseudomonas* species. We exposed young adult wild-type (N2) or RNAi defective animals (*rde-*
226 *1(ne219)*) to exogenous Orsay virus and quantified the amount of virus present at 2 h and 24 h
227 post-exposure, with the difference in RNA levels at these points reflecting viral genome
228 replication. Animals of the RNAi defective *rde-1(ne219)* background have a defective antiviral
229 response leading to higher viral loads than wild-type animals[23]. The *rde-1(ne219)* mutant
230 therefore provides a more sensitive genetic background in which to detect viral replication
231 following rare infection events within a population as is expected in the presence of *P. aeruginosa*
232 PA14. In *rde-1(ne219)* animals viral RNA1 levels increased at 24 h relative to 2 h post exposure
233 regardless of the bacteria present (Fig. 3B and 3C). On the other hand, in the wild-type
234 background replication was not observed in animals exposed to *P. aeruginosa* PA14 and was

235 attenuated in animals exposed to *P. aeruginosa* PA01 compared to animals exposed to *E. coli*
236 OP50 or *P. lurida* MYb11 (Fig. 3B and 3C). In a wild-type background individuals exposed to *P.*
237 *aeruginosa* PA01 and *P. aeruginosa* PA14 are less likely to become infected from exogenous
238 Orsay virus (Fig. 2B and Supp. Fig. 5). It is therefore likely that the viral load we observed in the
239 wild-type populations is due to a smaller proportion of the population being infected, rather than
240 hampered replication[23].

241 We also assessed whether *P. lurida* MYb11, *P. aeruginosa* PA01, or *P. aeruginosa* PA14
242 was capable of rapidly degrading Orsay virus or preventing viral shedding, either of which might
243 account for attenuation of Orsay virus transmission. We did not observe a substantial decrease
244 in viral stability in the presence of any bacterium suggesting Orsay virus is not rapidly degraded
245 (Fig. 3D and 3E). We did observe an approximately 2-fold decrease in viral levels between *E. coli*
246 OP50 and *P. lurida* MYb11, however, this difference already existed within 30 min of exposure to
247 each bacterium and did not grow further over the course of 24 h suggesting we are measuring
248 differences in recovery of Orsay virus from each bacterial lawn, rather than enhanced
249 degradation in the presence of *P. lurid*a MYb11 (Fig. 3D and 3E). We measured rates of Orsay
250 virus shedding during a transmission assay. We did not observe a substantial decrease in viral
251 shedding in the presence of any bacterium (Fig. 3F). We observed approximately 4-fold lower
252 levels of Orsay virus shed in the presence of *P. lurida* MYb11 vs *E. coli* OP50, but as suggested by
253 our virus stability data, we believe these differences at least partly reflect differences in Orsay
254 virus recovery from each bacterial lawn rather than actual differences in viral shedding (Fig. 3F).
255

256 **Attenuation of Orsay virus transmission by *Pseudomonas* species is dependent on regulators**
257 **of bacterial quorum sensing.**

258 Extensive studies on *Pseudomonas* species have demonstrated the importance of quorum
259 sensing for regulating many community-level behaviors in response to growing population
260 density[48]. *P. aeruginosa* relies upon three quorum sensing systems: *las*, *rhl*, and *pqs*. These
261 systems are arranged hierarchically, however crosstalk between them is extensive (Fig. 4A)[48]. In
262 *P. aeruginosa*, an additional layer of regulation stems from two-component regulatory systems
263 such as *gacA/gacS* which regulates numerous genes that together influence quorum sensing,
264 virulence, and biofilm development (Fig. 4A)[49–51]. *P. aeruginosa* possesses three
265 exopolysaccharide biosynthetic clusters that each contribute to biofilm formation: *pel*, *psl*, and
266 *alg*. However, *P. aeruginosa* PA01 preferentially produces Psl while *P. aeruginosa* PA14 is unable
267 to synthesis Psl and produces Pel[52–56]. We hypothesized that quorum sensing might mediate the
268 effect of *Pseudomonas* strains to attenuate virus transmission, while differences in
269 exopolysaccharide production might mediate the enhanced attenuation of virus transmission
270 observed in the presence of *P. aeruginosa* PA14 compared with what was observed in the
271 presence of *P. aeruginosa* PA01. Therefore, we tested a panel of *P. aeruginosa* PA01 and *P.*
272 *aeruginosa* PA14 quorum sensing and biofilm mutants to determine whether quorum sensing or
273 biofilm formation was involved in the attenuation of Orsay virus infection mediated by *P.*
274 *aeruginosa.*

275 Mutations of any the regulators of the *las*, *rhl*, or *pqs* quorum sensing systems suppressed
276 the attenuation of Orsay virus infection caused by the presence of wild-type *P. aeruginosa* PA01
277 (Fig. 4B, Supp. Fig. 7). Knockout of *gacA* in *P. aeruginosa* PA01 also suppressed the attenuation
278 of Orsay virus infection (Fig. 4B, Supp. Fig. 7). On the other hand, mutation of any of the three

279 exopolysaccharide production pathways had no potent effect on the attenuation of infection (Fig.
280 4B, Supp. Fig. 7). These data support a role for quorum sensing regulated processes in reducing
281 Orsay virus infection rates but do not implicate a role for individual exopolysaccharides.

282 For *P. aeruginosa* PA14, mutation of *gacA* or *rhlR* suppressed the attenuation of Orsay
283 virus infection observed in the presence of wild-type *P. aeruginosa* PA14 (Fig. 4C, Supp. Fig. 8).
284 Loss of the *rhlR* regulators *rhlI* or *pqsE* alone had no effect on the attenuation of Orsay virus
285 infection, but simultaneous mutation of both *rhlI* and *pqsE* did suppress the attenuation of Orsay
286 virus infection observed in the presence of wild-type *P. aeruginosa* PA14, similar to that observed
287 for the *rhlR* mutant, suggesting *rhlI* and *pqsE* function redundantly to regulate *rhlR* in this context
288 (Fig. 4C, Supp. Fig. 8)[57]. Mutation of *lasI* or *lasR* suppressed the attenuation of Orsay virus
289 infection to a lesser extent (Fig. 4C, Supp. Fig. 8). Independent mutation of two genes responsible
290 for *pel* or *alg* exopolysaccharide production had no effect on infection rates (Fig. 4C, Supp. Fig.
291 8). We further confirmed that mutation of *rhlR* and *gacA* in *P. aeruginosa* PA01 or *P. aeruginosa*
292 PA14 suppressed the attenuation of Orsay virus infection via FISH (Fig. 4D and 4E). These data
293 suggest a role for quorum sensing in mediating *P. aeruginosa* PA14 suppression of Orsay virus
294 infection, as we observed for *P. aeruginosa* PA01. However, our results obtained in the presence
295 of *P. aeruginosa* PA14 suggest that there may be some differential regulation of the bacterial
296 effectors responsible in comparison to *P. aeruginosa* PA01, or additional non-quorum sensing
297 related factors that also mediate suppression.

298 As *P. aeruginosa* mutants could suppress the attenuation of infection observed by wild-
299 type *P. aeruginosa* in the presence of exogenous virus, we next confirmed that these *P.*
300 *aeruginosa* mutants similarly affected transmission from infected spreader animals. All *P.*

301 *aeruginosa* PA01 quorum sensing mutants suppressed the attenuation of transmission by
302 increasing the incidence proportion >6-fold compared to the wild-type *P. aeruginosa* PA01 (Fig.
303 4F). *P. aeruginosa* PA14 *rhlR* and *gacA* mutants suppressed the attenuation of transmission by
304 increasing the incidence proportion 19-fold and 17-fold respectively compared to wild-type *P.*
305 *aeruginosa* PA14, but a *lasI* mutant had minimal effect consistent with the pattern we observed
306 in the susceptibility assay using exogenous Orsay virus (Fig. 4F). Likewise, the magnitude of
307 suppression of the attenuation of Orsay virus transmission observed in the *P. aeruginosa rhlR* or
308 *gacA* mutants was greater in the *P. aeruginosa* PA01 background compared to the *P. aeruginosa*
309 PA14 background, potentially suggesting the existence of additional strain specific factors that
310 act in *P. aeruginosa* PA14 to attenuate Orsay virus transmission.

311 Our findings suggest the possibility that quorum sensing molecules could act directly to
312 attenuate infection. To explore this hypothesis, we prepared liquid *E. coli* OP50, *O. vermis* MYb71,
313 *P. lurida* MYb11, *P. aeruginosa* PA01, and *P. aeruginosa* PA14 cultures and added culture
314 supernatant to plates containing *E. coli* OP50 and Orsay virus. We did not observe any potent
315 effect on host susceptibility to infection by Orsay virus from any supernatant (Supp. Fig. 9),
316 although it is difficult to rule out the possibility that the compounds may act at concentrations
317 that are locally higher than the concentrations at which the compounds are present in our
318 experiments.

319

320 ***P. aeruginosa* genes linked to virulence reduce Orsay virus transmission and infection.**

321 We designed a candidate-based screen using a non-redundant transposon insertion
322 library to gain further insight into the genetic regulation of *P. aeruginosa* mediated reduction of

323 Orsay virus transmission and infection (Fig. 5A)[58]. We identified candidate genes to include in our
324 screen from three sources: *gacA*-regulated genes, *rhlR*-regulated genes (but *rhlI*- or *pqsE*-
325 independent), and the set of genes required for full virulence in *C. elegans* previously identified
326 by Feinbaum et al. (Fig 5A)[51,59,60]. Of the 211 genes tested, 18 putative hits, including *lasI*, *rhlR*,
327 and *gacA*, were identified with the corresponding *P. aeruginosa* PA14 mutants exhibiting
328 suppression of the attenuation of Orsay virus infection by wild-type *P. aeruginosa* PA14 (Fig. 6A,
329 Supp. Table 3). Using the 15 novel candidate genes, we performed an additional set of
330 susceptibility assays which confirmed six of the hits (Fig. 5B, Supp. Fig. 10, Supp. Table 3). The
331 identified hits grouped into two clusters based on the strength of their suppression. Transposon
332 insertion in the genes *ptsP*, *prpC*, and *kinB* led to marked suppression of the attenuation of Orsay
333 virus leading to infection of 97%, 89%, and 82% of the population respectively compared to
334 infection in only 4.2% of the population in the presence of wild-type *P. aeruginosa* PA14 (Fig. 5B,
335 Supp. Fig. 10). Transposon insertion in three additional genes, *clpA*, *glnK*, and *fabF1* resulted in
336 weaker, but robust suppression of the attenuation of Orsay virus leading to infection of 34%,
337 28%, and 17% of the population respectively (Fig 5B, Supp. Fig. 10). We additionally tested
338 whether transposon insertion into these genes suppressed attenuation of Orsay virus
339 transmission. While we observed a trend towards mutations affecting susceptibility also affecting
340 virus transmission, we observed a high degree of variation in the transmission assay, such that
341 only mutation of *ptsP* led to statistically significant suppression of Orsay virus attenuation (Fig.
342 5C).

343 We noted that all six of the hits originated from the set of genes required for full *P.*
344 *aeruginosa* PA14 virulence in *C. elegans*[60]. These hits represented only six out of the 41 tested

345 genes that are known to influence virulence, indicative of some degree of specificity in the
346 consequences of these mutations beyond their general effect on *P. aeruginosa* PA14 virulence[60].
347

348 ***P. lurida* MYb11 *gacA* is required for attenuation of Orsay virus transmission.**

349 We next sought to determine whether our findings from the interaction of *C. elegans* and
350 Orsay virus in the presence of *P. aeruginosa* could inform us further regarding the mechanisms
351 underlying the attenuation of Orsay virus transmission in the presence of *P. lurida* MYb11. In
352 particular, we identified *gacA, ptsP, prpC, and kinB* orthologs using Orthovenn2 and generated a
353 putative knockout allele of each gene by removing the coding potential for all but 10 amino acids
354 from the N and C termini (Fig. 6A)[61]. Following exposure to exogenous Orsay virus, knockout of
355 *gacA* in *P. lurida* MYb11 led to infection of 77% of the population compared to infection of 43%
356 of the population in the presence of wild-type *P. lurida* MYb11 from exogenous Orsay virus (Fig.
357 6B, Supp. Fig. 11A and 11B). These observations were confirmed via FISH, as the *gacA* mutant
358 supported infection of 62% of the population versus 37% infection in the presence of wild-type
359 *P. lurida* MYb11 (Fig. 6C). The *gacA* mutation also suppressed the attenuation of Orsay virus
360 transmission, increasing the incidence proportion 2.9-fold compared to wild-type *P. lurida*
361 MYb11 (Fig. 6D). These data suggest that *gacA* has a conserved role between *P. aeruginosa* and
362 *P. lurida* MYb11 in the attenuation of Orsay virus transmission and infection of *C. elegans*. On the
363 other hand, knockout of the *P. lurida* MYb11 orthologs of *ptsP*, *prpC*, or *kinB* failed to suppress
364 the attenuation of Orsay virus infection or transmission by *P. lurida* MYb11 (Fig. 6E, Supp. Fig.
365 11C and 11D)[60,62]. One explanation of these results is that these genes play different roles within
366 *P. lurida* MYb11 and *P. aeruginosa* and therefore their mutation did not have the same

367 consequences for Orsay virus attenuation. Alternatively, these results might suggest that *ptsP*,
368 *prpC*, and *kinB* act to attenuate Orsay virus infection via some specific effect on *P. aeruginosa*
369 PA14 virulence but do not influence the interaction of *P. lurida* MYb11 with *C. elegans*.
370
371 ***O. vermis* MYb71 closely interacts with the *C. elegans* intestinal brush border.**
372 *P. lurida* MYb11 and *O. vermis* MYb71 can both be isolated from *C. elegans* natural
373 environment[36,39]. We were therefore curious how exposure to both bacteria simultaneously
374 would impact Orsay virus infection rates. When cultures of *O. vermis* MYb71 and *P. lurida* MYb11
375 were concentrated to 25mg/mL and then mixed, we observed that a 50% mixture of each
376 bacterium (v:v) attenuated infection to the same degree as pure *P. lurida* MYb11 (Fig. 7A, Supp.
377 Fig. 11A-B). Moreover, we also noted that mixing *O. vermis* MYb71 with *E. coli* OP50 also lead to
378 infection rates similar to pure *E. coli* OP50 (Fig. 7A, Supp. Fig. 11A-B). Previous studies have
379 identified that *Ochrobactrum* is found in large numbers in the *C. elegans* intestine following
380 exposure[36,39]. We investigated how the levels of *Ochrobactrum* in the intestine changed following
381 exposure to pure or mixed lawns of bacteria. When alone, GFP expressing *Ochrobactrum* BH3
382 was readily observed within the intestine at 4 or 24 h of exposure. Interestingly, exposure to a
383 mixed lawn of *Ochrobactrum* BH3 and *P. lurida* MYb11 reduced intestinal accumulation of
384 *Ochrobactrum* BH3 compared to the pure *Ochrobactrum* BH3 treatment (Fig 7B and 7C, Supp Fig.
385 11C-F). On the other hand, exposure to a mixed lawn of Ochrobactrum BH3 and *E. coli* OP50
386 reduced accumulation of *Ochrobactrum* BH3 at four hours compared to a pure *Ochrobactrum*
387 BH3 treatment, but this difference was minimal by 24 hours (Fig 7B and 7C, Supp Fig. 11C-F).

388 These data suggested that the presence of *Ochrobactrum* in the intestine may be important
389 for its ability to promote Orsay virus infection. We therefore fixed *C. elegans* exposed to *O. vermis*
390 MYb71 or *E. coli* OP50 for examination via electron microscopy and imaged cross sections of the
391 intestine. As expected from our fluorescence experiments, *O. vermis* MYb71 was readily
392 observed in the intestinal lumen at 4 or 24 h of exposure (Fig. 7D and 7E). The glycocalyx is the
393 mucus-like layer covering *C. elegans* intestinal cells and that recent work has suggested may play
394 a role in defense against Orsay virus[63,64]. The glycocalyx of animals exposed to *O. vermis* MYb71
395 was observed with regions of variable thickness and potential instances of *O. vermis* MYb71
396 deforming the microvilli brush border as opposed to animals exposed to *E. coli* OP50 where the
397 glycocalyx appeared uniform and undisturbed (Fig. 7D and 7E). A recent report observed that
398 *Serratia marcescens* promoted infection of the mosquito *Aedes aegypti* by Dengue, Zika, and
399 Sindbis viruses by secreting a protein, enhancin, that degrades the mucus layer covering
400 epithelial cells[14]. These observations lead us to speculate that *O. vermis* MYb71 mediated
401 disruption of the brush border and glycocalyx promotes Orsay virus infection although this
402 hypothesis has yet to be tested.
403
404 **Discussion**
405 In our study, we quantitatively define the effect of bacteria on the transmission of Orsay
406 virus in the *C. elegans* host. While the presence of *O. vermis* MYb71 enhanced the transmission
407 of Orsay virus, the presence of *P. lurida* MYb11 or *P. aeruginosa* strains PA01 and PA14
408 attenuated Orsay virus transmission. The enhancement of Orsay virus transmission by *O. vermis*
409 MYb71 and reduction of transmission by *P. lurida* MYb11 and *P. aeruginosa* PA01 and PA14 was

410 mirrored in assays assessing infection rates by exogenous virus. Our results using exogenous virus
411 demonstrate that host susceptibility to Orsay virus infection may vary by over three orders of
412 magnitude in the presence of *O. vermis* MYb71 versus *P. lurida* MYb11 which are found in the
413 natural environment in association with *C. elegans*[36,39]. Moreover, we observe that pathogenic
414 *P. aeruginosa*, which may be found in natural environments, can further attenuate Orsay virus
415 transmission[31]. Our work is also consistent with a recent study by González and Félix that also
416 reported that monoaxenic cultures of other bacteria from the environment of *C. elegans* impact
417 host susceptibility[65].

418 Our observations that two *Ochrobactrum* species promoted transmission of Orsay virus
419 are intriguing given that other *Ochrobactrum* species have also been linked to viral infections.
420 *Ochrobactrum intermedium* promoted poliovirus infection in mice and enhanced poliovirus
421 stability in vitro[13]. *Ochrobactrum anthropi*, an opportunistic human pathogen, was identified
422 using a random forest analysis as one of the most predictive features differentiating the upper
423 respiratory tract of human patients recovering from influenza infection versus healthy controls[66].
424 Our observations in the *C. elegans* host raise the speculative possibility that *Ochrobactrum*
425 colonization may have roles in evolutionarily diverse hosts in modulating viral infection. Further,
426 our electron micrographs point to an intriguing hypothesis that *Ochrobactrum* disrupts the brush
427 border region of epithelial cells thereby promoting viral infection. Such a mechanism would be
428 consistent with recent work identifying that *Serratia marcescens* produces the protein enhancin,
429 which promotes viral infection by degrading the mucus layer covering epithelial cells in the
430 mosquito *Aedes aegypti*[14]. Additional work will need to be performed to explicitly test whether

431 such a mechanism is at play in *Ochrobactrum* mediated enhancement of Orsay virus infection
432 and transmission.

433 *P. lurida* MYb11 and *P. aeruginosa* PA01 and PA14 shared the ability to attenuate Orsay
434 virus infection and transmission. *P. lurida* MYb11 promotes developmental rate and fitness at a
435 cost to overall lifespan[39,46]. In contrast, *P. aeruginosa* rapidly kills *C. elegans* and is detrimental to
436 host fitness[30,44]. Under our experimental conditions exposure to all three shortened lifespan
437 compared to exposure to *E. coli* OP50. Given that *O. vermis* MYb71 shortened lifespan to the
438 same extent as *P. aeruginosa* PA14 but had the opposite effect on host susceptibility to Orsay
439 virus, we do not believe that general virulence by any bacterium is responsible for the observed
440 effects on host susceptibility. Rather, unique virulence processes specific to each bacterium may
441 contribute to the unique effects of each bacterium on host susceptibility to Orsay virus.

442 We identified that *gacA* regulates the attenuation of Orsay virus by *P. aeruginosa* PA01
443 and PA14 and *P. lurida* MYb11. In Pseudomonads, *gacA/gacS* regulate processes related to
444 quorum sensing and virulence[67]. Quorum signaling influences additional aspects of *P. aeruginosa*
445 physiology, including swarming behaviors, biofilm formation, secondary metabolism rates, and
446 overall transcription patterns[48]. To gain additional insights into the *P. aeruginosa* PA14 effects on
447 Orsay virus transmission we conducted a candidate-based screen of genes influenced by quorum
448 signaling and genes that regulate virulence towards *C. elegans*[51,59,60]. We identified six additional
449 genes, *ptsP*, *prpC*, *kinB*, *clpA*, *glnK*, and *fabF1,* that when mutated suppressed *P. aeruginosa* PA14
450 attenuation of Orsay virus infection. Each of these genes, in addition to *gacA*, *rhlR*, and *lasI* has
451 been shown to be required for full *P. aeruginosa* PA14 virulence in *C. elegans*[60]. However, we
452 observed that only these six out of the total 41 virulence-related genes identified in Feinbaum *et*

453 *al*. influenced Orsay virus infection, arguing further against a role for general virulence in the
454 attenuation of Orsay virus transmission and infection caused by *P. aeruginosa* PA14 and *P.*
455 *aeruginosa* PA01[60]. Additionally, while mutation of the *ptsP*, *prpC*, and *kinB* orthologs of *P. lurida*
456 MYb11 failed to suppress the attenuation of Orsay virus, it is unclear whether these genes
457 influence the effect of *P. lurida* MYb11 on host lifespan or even whether *P. lurida* MYb11
458 pathogenicity mediated by other factors leads to attenuation of Orsay virus infection.

459 *C. elegans* is unlikely to associate with a single bacterium in its natural environment.
460 However, *C. elegans* shows clear behavioral preferences for grazing on certain bacteria from its
461 environment and may eat monoxenic lawns in the wild[68]. Our data demonstrate that individual
462 bacteria can have a profound impact on Orsay virus transmission rates in a species-specific
463 manner. Additionally, the tractability of the *C. elegans*-Orsay virus experimental system allowed
464 us to identify molecular determinants of viral transmission and will be useful for identifying
465 additional biotic factors that influence viral transmission. Our work builds on the expanding body
466 of knowledge showing that the microbiota can influence the interactions between viruses and
467 their animal hosts.

468

469 **Materials and methods**

470

471 *C. elegans* strains and growth conditions

472 *C. elegans* were maintained on NGM agar plates (17 g agar, 2.5 g peptone, 3 g NaCl per 1 L water)

473 containing *E. coli* OP50[41]. Strains bearing the *glp-4(bn2)* temperature sensitive mutation were

474 maintained at 16°C, while all other were maintained at 20°C. All assays were performed on SKA

475 assay plates at 20°C (17 g agar, 3.5 g peptone, 3 g NaCl per 1 L water)[30]. A full list of *C. elegans*

476 strains used in this study is contained within the Supplement (Supplement Table 1). For all assays

477 relying upon *pals-5p::GFP*, induction was manually assessed using a Nikon SMZ18

478 stereofluorescent microscope.

479

480 Bacterial strains and growth conditions

481 All bacteria were grown in Luria broth (10 g tryptone, 5 g yeast, 10 g NaCl per 1 L water). *E. coli*

482 OP50 and *P. aeruginosa* strains were grown at 37°C with shaking, while all other strains were

483 grown at 27°C with shaking. A full list of bacterial strains used in this study is contained within

484 the Supplemental Information (Supplement Table 2).

485

486 Orsay virus isolation and batch testing

487 Orsay virus was isolated from infected WUM31(*rde-1(ne219);jyIs9[pals-5p::gfp;myo-*

488 *2p::mCherry]*) individuals. Plates with gravid WUM31 were bleached to obtain eggs. Eggs were

489 hatched overnight in M9 solution rotating at 20°C and the L1 larvae were arrested to synchronize

490 the population. L1 larvae were combined with 100 μL of 6x concentrated *E. coli* OP50 liquid
491 culture and 50 μL of Orsay virus filtrate, plated on SKA plates, and once dried, placed at 20°C for
492 48 h. Four GFP positive individuals were then transferred to a new 6cm NGM plate with *E. coli*
493 OP50 and maintained until just starved. Twenty such 6cm plates were washed with 10 mL of M9
494 and the resulting suspension was Dounce homogenized. Alternatively, two 3.5 cm SKA plates
495 containing infected WUM31 animals were allowed to starve and then equally chunked onto eight
496 10 cm NGM plates with *E coli* OP50. Once these plates were just starved, the plates were washed
497 with 10 mL of M9 and homogenized as above. The homogenized suspension was then centrifuged
498 at 13,200xg for five min. The supernatant was passed through a 0.22 μm filter and aliquoted.
499 Each batch of virus was tested for potency and an ID_{50} calculated for ZD2611 populations in the
500 presence of *E. coli* OP50 (Supp. Fig. 2). On average, 3.6 μL of Orsay virus stock prepared as
501 indicated in the Methods was required to infect 50% of a population of ZD2611 animals in the
502 presence of *E. coli* OP50 after 24 hours (Supp. Fig. 2). We observed variability in the measured
503 ID_{50} even when using the same batch of Orsay virus (e.g. Fig. 1D vs Supp. Fig. 3A vs. Supp. Fig.
504 3B). We therefore chose to control all our experiments internally rather than attempt to
505 normalize between Orsay virus batches and we report doses used in arbitrary units (a.u.),
506 however 1 a.u. corresponds to 1 μL of Orsay virus filtrate.
507
508 <u>Preparation of Uninfected Individuals for transmission and susceptibility assays</u>
509 Prior to all assays, plates with fecund ZD2611(*glp-4(bn-2);jyIs8[pals-5p::gfp;myo-2p::mCherry]*)
510 were bleached to obtain eggs. Eggs were hatched overnight in M9 solution rotating at 20°C and
511 the L1 larvae were arrested to synchronize the population. ZD2611 L1s were dropped onto plates

512 containing *E. coli* OP50 and placed at 20°C for 64-72 h. At this temperature reproduction is
513 delayed, but not eliminated, and no L1s are observed during transmission or susceptibility assays.
514 The resulting young adults were washed off the plates in M9 and centrifuged at 1000xg for one
515 minute. After removing the supernatant, the young adults were once again washed in M9, then
516 centrifuged at 1000 x g for one minute. Young adults were directly dropped onto prepared plates
517 described below.
518
519 Preparation of Bacteria for transmission and susceptibility assays
520 Unless otherwise indicated, bacteria were cultured overnight and added to cover the assay
521 plates. Plates containing *E. coli* OP50 or *P. aeruginosa* strains were placed at 37°C for 24 h. Plates
522 containing *O. vermis* MYb71 or *P. lurida* MYb11 strains were placed at 25°C for 24 h. All plates
523 were then moved to room temperature for an additional 24 h before the addition of virus.
524
525 For the natural isolate transmission screen and early transmission assay cultures were grown to
526 late stationary phase. Cultures were then spun down for six minutes at 4000xg and reconstituted
527 to 25 mg/mL in their own supernatant. 150 μL of this suspension was combined with 50 μL of a
528 mix of M9 for transmission assays or 50 μL of a combination of Orsay virus filtrate and M9 for the
529 early transmission assay. This mixture was combined with young adult ZD2611 individuals and
530 directly added to cover assay plates before drying.
531
532 Transmission assays

533 To obtain infected spreader animals, fecund ZD2610 (*glp-4(bn-20); rde-1(ne219); jyIs8[pals-*
534 *5p::gfp;myo-2p::mCherry]*) were bleached to obtain eggs. Eggs were hatched overnight in M9
535 solution rotating at 20°C and the L1 larvae were arrested to synchronize the population. Arrested
536 ZD2610 L1s were dropped onto NGM plates containing *E. coli* OP50 and placed at 20°C for 48 h.
537 Animals were then washed off the plates in M9 and centrifuged at 1000xg for one min. After
538 removing the supernatant, the young adults were washed with M9 again then centrifuged at
539 1000xg for one min. Supernatant was once again removed, and individuals were immediately
540 mixed with 100 μL of 6x overnight *E. coli* OP50 culture and 50 μL of Orsay virus for a minimum of
541 18-20 h. *pals-5p::GFP*-positive ZD2610 young adults were identified and picked onto transfer
542 plates containing the appropriate bacteria prepared as indicated above for 4-6 h. After this
543 period, five spreaders were transferred to assay plates containing the same bacteria and
544 approximately 100 uninfected ZD2611 individuals to start the assay. Transmission assays were
545 scored 24 h after adding spreader individuals.
546
547 For the natural isolate transmission screen, arrested ZD2610 L1s were combined with 100 μL of
548 6x concentrated *E. coli* OP50 and 50 μL of Orsay virus filtrate and once dried, placed at 20°C for
549 64-72 h. On the day of the assay, *pals-5p::GFP*-positive ZD2610 young adults were identified and
550 picked onto transfer plates containing the appropriate bacteria prepared as indicated above for
551 4-6 h. After this period, five spreaders were transferred to assay plates containing the same
552 bacteria and approximately 100 uninfected ZD2611 individuals to start the assay.
553
554 <u>Incidence proportion</u>

555 Incidence proportion was calculated by dividing the number of newly infected animals by the
556 total non-spreader population per plate. Individual plates for which the total number of *pals-*
557 *5p::GFP* positive individuals after 24 h was less than the initial number of spreaders placed on the
558 plate were excluded to eliminate potential differences in incidence proportion caused by unequal
559 numbers of infected spreader animals. For Fig. 1C a single plate was censored from *P. lurida*
560 MYb11, for Fig. 2A six plates were censored from *P. aeruginosa* PA14, and for Fig. 4E 12 plates
561 were censored: seven from *P. aeruginosa* PA14, three from *P. aeruginosa* PA01, one from *P.*
562 *aeruginosa* PA14Δ*gacA* , and one from *P. aeruginosa* PA14Δ*lasI.*
563
564 Susceptibility assays
565 Unless otherwise indicated, Orsay virus filtrate at the indicated doses was diluted in filtered M9
566 solution. 200 μL total was applied to each assay plate and swirled to cover the entire bacterial
567 lawn. Plates were then dried before the addition of approximately 100 uninfected ZD2611
568 individuals prepared as indicated above. Assays were scored 24 h later using a Nikon SMZ18
569 stereo fluorescent microscope and the fraction of *pals-5p::GFP*-positive individuals was
570 calculated.
571
572 Early Transmission Assay
573 For early transmission assay, young ZD2611 adults were exposed to 0 a.u. or 5 a.u. exogenous
574 Orsay virus in the presence of *O. vermis* MYb71. 8 hours post infection five infected individuals
575 from the 5 a.u. plate were transferred to the 0 a.u. plate to assess whether transmission from
576 these individuals would occur. Both plates were scored 16 hours after the transfer.

577

578 Supernatant Transfer Assay

579 Assay plates were prepared with *E. coli* OP50 for susceptibility assays as indicated above. Bacteria
580 were inoculated into 6 mL of LB and allowed to grow for 48 h. Cultures were then spun at 4,000xg
581 for 6 minutes and the spent media supernatant was passed through a 0.22 μm filter. 200 μL of
582 the filtered supernatant was added to the *E. coli* OP50 assay plates just prior to the addition of
583 Orsay virus and ZD2611 young adults.

584

585 Fluorescence *in situ* hybridization

586 Previously published probes were obtained to target the RNA1 segment of Orsay virus[25]. Animals
587 were infected according to the methods described above for susceptibility assays. Animals were
588 processed according to the Stellaris RNA FISH Protocol for *C. elegans* (LGC Biosearch
589 Technologies) with minor modifications. Briefly, young adults were washed off the plate and
590 rinsed twice in M9. Animals were then fixed for 30 min rotating in a microcentrifuge tube at 20°C.
591 After washing twice with 1 mL of phosphate buffered saline animals were permeabilized in 70%
592 of ethanol and stored at 4°C for 1-7 d. Animals were washed with Wash Buffer A before addition
593 of 100 μL of hybridization buffer containing 3 μL of RNA1 probe mix. Probe was hybridized
594 overnight at 46°C. Animals were then washed with Wash Buffer A alone once, and then again
595 with Wash Buffer A containing 5 ng/mL DAPI. Lastly 100 μL of Wash Buffer B was added before
596 mounting animals on slides with 25 μL of Vectashield Mounting Medium. The fraction of
597 individuals with RNA1 staining was then quantified using a Nikon SMZ18 stereofluorescent
598 microscope or a Zeiss AxioImager Z1 compound fluorescent microscope.

599

600 Viral Stability

601 Assay plates with each bacterium were prepared as described above. 50 a.u. Orsay virus was
602 added to each plate as in a susceptibility assay however no *C. elegans* were added. Plates were
603 washed with 1 mL of ddH_20 after 30 minutes or 24 h. A spike-in control was also included where
604 50 a.u. of Orsay virus was directly added to 1ml H_20 and processed the same as all other samples.
605 The resulting mixture was spun at 15000 rpm (max speed) at 4°C for 10 min. 1 μl of the
606 supernatant was used to make cDNA (Promega GoScript reverse transcriptase using random
607 primers (A2801)). Orsay virus RNA1 level was quantified by qPCR using 1 μl of 1/5 diluted cDNA
608 (GoTaq Promega A6001) and run on QuantStudio 3 Real Time PCR system (RNA1 qPCR primers
609 GW194 and GW195)[23].

610 Viral Shedding

611 Infected ZD2610 animals were prepared as indicated above with infection occurring at the L4
612 stage. 24 h later as young adults, 20 *pals-5p::GFP* positive animals were transferred to assay
613 plates prepared with bacteria as indicated above for a transmission assay. These animals were
614 allowed to shed virus onto the plate for 24 h at 20°C. Spreaders were then removed and the assay
615 plates were washed with 1 mL of M9. The resulting mixture was spun at 15000 rpm (max speed)
616 at 4°C for 10 min. 1 μl of the supernatant was used to make cDNA (Promega GoScript reverse
617 transcriptase using random primers (A2801)). Orsay Virus RNA1 level was quantified by qPCR
618 using 1 μl of 1/5 diluted cDNA (GoTaq Promega A6001) and run on QuantStudio 3 Real Time PCR
619 system. (RNA1 qPCR primers GW194 and GW195)[23]

620 RNA Extraction

621 Animals were washed 5 times in M9 and collected in TRIzol reagent (Invitrogen) and stored at -
622 80°C before extraction. RNA extraction was performed using Direct-zol RNA microprep kits (Zymo
623 Research) following the manufacturer's instructions.

624 qPCR

625 cDNA was made using 1000 ng of RNA as template (Promega GoScript Reverse Transcriptase
626 using Random Primers). cDNA was diluted at 1/80 and qPCR were performed using 1 μl of diluted
627 cDNA (GoTaq Promega) and run on QuantStudio 3 Real Time PCR system. RNA1 levels were then
628 quantified via qPCR using previously published primers[23]. Orsay virus RNA levels were normalized
629 to the internal control host gene snb-1 (primers GCTCAGGTTGATGAAGTCGTC and
630 GGTGGCCGCAGATTTCTC).

631 Plasmid-based replication experiments

632 Adult animals carrying a transgene containing the wild-type RNA1 or RNA1D601A Orsay virus
633 genome segment under the control of a heat-inducible promoter were placed on the indicated
634 bacteria for 4 h before heat-shock at 33°C for 2 h[47]. Animals then recovered at 20°C for 20 h
635 before harvesting for RNA extraction and qPCR as detailed above. RNA1 levels were normalized
636 to the values obtained from animals bearing the wild-type RNA1 and exposed to *E. coli* OP50.

637 Orsay virus replication in the presence of *P. lurida* MYb11 and *P. aeruginosa*

638 Adult ERT54 (*jyIs8[pals-5p::gfp;myo-2p::mCherry]*) or WUM31 (*rde-1(ne219); jyIs8[pals-*
639 *5p::gfp;myo-2p::mCherry)*] were exposed to exogenous Orsay virus in the presence of *P. lurida*

640 MYb11, *P. aeruginosa* PA01, or *P. aeruginosa* PA14 prepared as in a susceptibility assay. After 2
641 h or 24 h, animals were harvested for RNA extraction and qPCR as detailed above. RNA1 levels
642 were quantified via qPCR. Within each genotype, the data for each experiment were normalized
643 to the 2 h timepoint.

644 *P. lurida* MYb11 mutant construction

645 A protocol developed for allelic exchange in *P. aeruginosa* was modified for use in *P. lurida*
646 MYb11[69]. Briefly, homology arms flanking the region to be deleted were obtained using
647 polymerase chain reaction (PCR) and cloned into the pExG2-KanR suicide vector using Hi-Fi
648 Assembly (New England Biolabs)[70]. DH5α *E. coli* were transformed using a standard heat shock
649 protocol. Successful transformants were selected for on LB+Kanamycin (50 μg/mL) plates and
650 colony PCR was performed to check for proper insert size in the transformants. *E. coli* bearing
651 the desired plasmid were grown overnight in LB+Kanamycin (50 μg/mL). Plasmids were then
652 obtained using a Qiagen MiniPrep Kit (Qiagen). Plasmids were assessed for the desired sequence
653 by Sanger sequencing and transformed into *P. lurida* MYb11 using the following electroporation
654 procedure. *P. lurida* MYb11 was grown overnight then placed on ice for 30 min. The culture was
655 spun down at 4°C and washed twice with ice-cold water. After reconstitution in 100 μL of ice-
656 cold water the suspension was transferred to a pre-chilled cuvette and transformed at 630 kV
657 using an Eporator (Eppendorf). 900 μL of LB was added, and the suspension was transferred to a
658 microcentrifuge tube and incubated at 27°C for 2 h with shaking. The suspension was then plated
659 on LB+Kanamycin (50 μg/mL) plates and grown for 48 h at 25 °C. Colonies were picked and grown
660 overnight in LB. Cultures were streaked onto sucrose plates (15 g agar, 10 g tryptone, 5 g yeast,

661 60 g sucrose per 1 L water) to perform sucrose-based counter selection[69]. Colonies that survived
662 were genotyped for the expected deletion.
663
664 Lifespan Analysis
665 Assay plates, bacteria, and ZD2611 animals were prepared as indicated above, however plates
666 were prepared with the addition of 50 μg of 5-fluorodeoxyuridine (FUdR) to eliminate the need
667 to transfer animals during the assay by preventing reproduction. 30 young adult ZD2611 animals
668 were added to each assay plate and assessed for survival every 24 h. Three replicate plates were
669 prepared per experiment and three experiments were performed in total.
670
671 Pumping Rate
672 Assay plates, bacteria, and ZD2611 animals were prepared as indicated above. 20 young adult
673 ZD2611 animals were transferred to each assay plate. At 6 h and 24 h, animals were recorded
674 with slow-motion video capture (1/4x) while feeding. Cycles of pharyngeal pumping were
675 counted and used to calculate the number of pharyngeal pumps per minute.
676
677 Mixing Susceptibility Assays and Colonization Assays
678 Bacteria were grown in LB for 48 h before being spun down at 4,000xg for 6 min. The resulting
679 cell pellets were weighed and reconstituted to 25 mg/mL in their own culture supernatant.
680 Concentrated bacteria were then combined with filtered M9 for colonization experiments or
681 filtered M9 plus 1 μL of Orsay filtrate for mixing susceptibility assays. For mixing susceptibility
682 assays young adult ZD2611 individuals prepared as above were added to the mixture before

683 addition to plates such that the bacterial lawn covered the entire plate. For colonization assays
684 N2 animals were prepared in the same manner to adulthood. Mixing susceptibility assays were
685 scored as a susceptibility assay as indicated above. Colonization assays were scored at 4 h or 24
686 h. Briefly, animals were picked off of the plate and anaesthetized in sodium azide before
687 mounting on a microscope slide. Fluorescent images of the region of the intestinal lumen behind
688 the pharynx were imaged using a Zeiss AxioImager Z.1 compound microscope. Images were then
689 imported into FIJI for analysis[71,72]. An irregular polygon tracing the region behind the pharynx
690 was drawn and the median fluorescence intensity measured.
691
692 Electron Microscopy
693 Animals were prepared for electron microscopy as indicated above for susceptibility assays.
694 Animals were washed off their plates in M9 and allowed to pellet by gravity. The supernatant
695 was removed and animals were anesthetized with sodium azide. Animals were then pipetted
696 into a type A 6mm Cu/Au carrier (Leica) and frozen in a high- pressure freezer (EM ICE, Leica).
697 This was followed by the following freeze-substitution protocol: (EM AFS2, Leica)
698 **Freeze substitution protocol:**
699 Cocktail 1: 2% osmium tetroxide, 0.1% uranyl acetate in anhydrous acetone
700 **PROGRAM:**

Cocktail	Temperature (start)	Temperature (end)	Time
Cocktail 1	-90 °C	-90 °C	60 h
Cocktail 1	-90 °C	-20 °C	11 h
Cocktail 1	-20 °C	-20 °C	10 h

Cocktail 1	-20 °C	0 °C	12 h
Acetone wash (4x)	0 °C	22 °C	2 h

701

702 After the washes in acetone, samples were incubated in propylene oxide for 30 min, then

703 slowly infiltrated in TAAB Epon (TAAB Laboratories Equipment Ltd, https://taab.co.uk) as

704 follows:

705

706 3:1 Propylene Oxide:TAAB Epon - 3hrs at RT

707 1:1 Propylene Oxide:TAAB Epon – ON at 4C

708 1:3 Propylene Oxide:TAAB Epon – 4 hrs at RT

709 100% TAAB Epon – 2 hrs at RT

710

711 Samples were embedded in fresh TAAB Epon and polymerized at 60 degrees C for 48 hrs.

712

713 Ultrathin sections (about 80nm) were cut on a Reichert Ultracut-S microtome, picked up on to

714 formvar/carbon coated copper grids, sections were stained with 0.2% lead citrate. The sections

715 were examined in a JEOL 1200EX Transmission electron microscope and images were recorded

716 with an AMT 2k CCD camera.

717

718 Data visualization and statistics

719 All experiments were performed three times. For transmission, qPCR, FISH-based susceptibility

720 assays, and lifespan assays data from each experiment are combined. For susceptibility assays

721 and colonization assays a single representative experiment is shown and replicates are shown in
722 the supplementary material. Data were analyzed in R Studio[73]. When comparing all the means of
723 more than two groups p-values were calculated using one-way ANOVA followed by the Tukey
724 HSD test. When comparing multiple experimental groups to a control group p-values were
725 calculated using one-way ANOVA followed by Dunnett's test. P-values for assays comparing only
726 two groups were calculated using Student's t-test or Welch's t-test as indicated. *E. coli* OP50 is
727 included in all experiments as a reference but was not included for statistical comparison unless
728 explicitly noted. Susceptibility assay curves were modeled using the drc[74] package in R. A two-
729 parameter log-logistic function was used to model the curve and ID_{50} values were calculated
730 using the ED function. Kaplan-Meier survival curves were made using the survival[75] package and
731 curves were compared using the log-rank test within the survdiff function. Plots were made using
732 the gdata[76], scales[77], drc[74], Rmisc[78], multcomp[79], survival[75], ggplot2[80], ggsignif[81], and cowplot[82]
733 packages.
734

735 **Acknowledgements**

736 We would like to thank members of the Kim/Fischer laboratory for helpful comments during
737 the preparation of this work. We would like to thank David Wang, Emily Troemel, Marie-Anne
738 Félix, Eliana Drenkard, Simon Dove, E. Peter Greenberg, Matthew Parsek, Jon Paczkowski, and
739 Read Pukkila-Worley for kindly providing strains. Some strains were provided by the CGC, which
740 is funded by NIH Office of Research Infrastructure Programs (P40 OD010440). We would like to
741 further thank Brendan O'Hara, Michael Gebhardt, and Simon Dove for assistance developing
742 the *P. lurida* MYb11 transformation protocol. Electron microscopy consultation, sample fixing,

743 and sample sectioning were performed in the HMS Electron Microscopy Facilty by Maria
744 Ericsson and Anja Nordstrom. We additionally thank Rita Droste (MIT) for assistance with
745 electron microscopy. B.G.V. was partially supported by the MIT Department of Biology
746 Graduate Program. B.G.V., N.S., S.E.J.F., and D.H.K were supported by NIH Grant
747 R35GM141794.

748 **References**

749 1. Edwards, R. A. & Rohwer, F. Viral metagenomics. *Nat Rev Microbiol* **3**, 504–510 (2005).
750 2. Srinivasiah, S. *et al.* Phages across the biosphere: contrasts of viruses in soil and aquatic
751 environments. *Res Microbiol* **159**, 349–357 (2008).
752 3. Pica, N. & Bouvier, N. M. Environmental factors affecting the transmission of respiratory
753 viruses. *Curr Opin Virol* **2**, 90–95 (2012).
754 4. Thangavel, R. R. & Bouvier, N. M. Animal models for influenza virus pathogenesis,
755 transmission, and immunology. *J Immunol Methods* **410**, 60–79 (2014).
756 5. de Vries, R. D. *et al.* Animal models of SARS-CoV-2 transmission. *Curr Opin Virol* **50**, 8–16
757 (2021).
758 6. Lowen, A. C., Mubareka, S., Steel, J. & Palese, P. Influenza Virus Transmission Is
759 Dependent on Relative Humidity and Temperature. *PLoS Pathog* **3**, e151 (2007).
760 7. SCHULMAN, J. L. & KILBOURNE, E. D. Airborne Transmission of Influenza Virus Infection
761 in Mice. *Nature* **195**, 1129–1130 (1962).
762 8. Quinn, T. C. *et al.* Viral Load and Heterosexual Transmission of Human Immunodeficiency
763 Virus Type 1. *New England Journal of Medicine* **342**, 921–929 (2000).
764 9. Edenborough, K. M., Gilbertson, B. P. & Brown, L. E. A Mouse Model for the Study of
765 Contact-Dependent Transmission of Influenza A Virus and the Factors That Govern
766 Transmissibility. *J Virol* **86**, 12544–12551 (2012).
767 10. Price, G. E., Lo, C.-Y., Misplon, J. A. & Epstein, S. L. Mucosal Immunization with a
768 Candidate Universal Influenza Vaccine Reduces Virus Transmission in a Mouse Model. *J*
769 *Virol* **88**, 6019–6030 (2014).
770 11. Chua, B. Y. *et al.* Inactivated Influenza Vaccine That Provides Rapid, Innate-Immune-
771 System-Mediated Protection and Subsequent Long-Term Adaptive Immunity. *mBio* **6**,
772 (2015).
773 12. Kane, M. *et al.* Successful Transmission of a Retrovirus Depends on the Commensal
774 Microbiota. *Science (1979)* **334**, 245–249 (2011).
775 13. Kuss, S. K. *et al.* Intestinal Microbiota Promote Enteric Virus Replication and Systemic
776 Pathogenesis. *Science (1979)* **334**, 249–252 (2011).
777 14. Wu, P. *et al.* A Gut Commensal Bacterium Promotes Mosquito Permissiveness to
778 Arboviruses. *Cell Host Microbe* **25**, 101-112.e5 (2019).
779 15. Zheng, D., Liwinski, T. & Elinav, E. Interaction between microbiota and immunity in health
780 and disease. *Cell Res* **30**, 492–506 (2020).
781 16. Berger, A. K., Yi, H., Kearns, D. B. & Mainou, B. A. Bacteria and bacterial envelope
782 components enhance mammalian reovirus thermostability. *PLoS Pathog* **13**, e1006768
783 (2017).
784 17. Hedges, L. M., Brownlie, J. C., O'Neill, S. L. & Johnson, K. N. *Wolbachia* and Virus
785 Protection in Insects. *Science (1979)* **322**, 702–702 (2008).
786 18. Teixeira, L., Ferreira, Á. & Ashburner, M. The Bacterial Symbiont Wolbachia Induces
787 Resistance to RNA Viral Infections in Drosophila melanogaster. *PLoS Biol* **6**, e1000002
788 (2008).
789 19. Moreira, L. A. *et al.* A Wolbachia Symbiont in Aedes aegypti Limits Infection with Dengue,
790 Chikungunya, and Plasmodium. *Cell* **139**, 1268–1278 (2009).

20. Bian, G., Xu, Y., Lu, P., Xie, Y. & Xi, Z. The Endosymbiotic Bacterium Wolbachia Induces Resistance to Dengue Virus in Aedes aegypti. *PLoS Pathog* **6**, e1000833 (2010).
21. Pimentel, A. C., Cesar, C. S., Martins, M. & Cogni, R. The Antiviral Effects of the Symbiont Bacteria Wolbachia in Insects. *Front Immunol* **11**, (2021).
22. Schulenburg, H. & Félix, M.-A. The Natural Biotic Environment of *Caenorhabditis elegans*. *Genetics* **206**, 55–86 (2017).
23. Félix, M.-A. *et al.* Natural and Experimental Infection of Caenorhabditis Nematodes by Novel Viruses Related to Nodaviruses. *PLoS Biol* **9**, e1000586 (2011).
24. Félix, M.-A. & Wang, D. Natural Viruses of *Caenorhabditis* Nematodes. *Annu Rev Genet* **53**, 313–326 (2019).
25. Franz, C. J. *et al.* Orsay, Santeuil and Le Blanc viruses primarily infect intestinal cells in Caenorhabditis nematodes. *Virology* **448**, 255–264 (2014).
26. Sarkies, P., Ashe, A., Le Pen, J., McKie, M. A. & Miska, E. A. Competition between virus-derived and endogenous small RNAs regulates gene expression in *Caenorhabditis elegans*. *Genome Res* **23**, 1258–1270 (2013).
27. Bakowski, M. A. *et al.* Ubiquitin-Mediated Response to Microsporidia and Virus Infection in C. elegans. *PLoS Pathog* **10**, e1004200 (2014).
28. Chen, K., Franz, C. J., Jiang, H., Jiang, Y. & Wang, D. An evolutionarily conserved transcriptional response to viral infection in Caenorhabditis nematodes. *BMC Genomics* **18**, 303 (2017).
29. Le Pen, J. *et al.* Terminal uridylyltransferases target RNA viruses as part of the innate immune system. *Nat Struct Mol Biol* **25**, 778–786 (2018).
30. Tan, M.-W., Mahajan-Miklos, S. & Ausubel, F. M. Killing of *Caenorhabditis elegans* by *Pseudomonas aeruginosa* used to model mammalian bacterial pathogenesis. *Proceedings of the National Academy of Sciences* **96**, 715–720 (1999).
31. Crone, S. *et al.* The environmental occurrence of *Pseudomonas aeruginosa*. *APMIS* **128**, 220–231 (2020).
32. Pelegrin, A. C. *et al. Pseudomonas aeruginosa* : a clinical and genomics update. *FEMS Microbiol Rev* **45**, (2021).
33. Kim, D. H. *et al.* A Conserved p38 MAP Kinase Pathway in *Caenorhabditis elegans* Innate Immunity. *Science (1979)* **297**, 623–626 (2002).
34. Kim, D. H. & Ewbank, J. J. Signaling in the innate immune response. *WormBook* 1–35 (2018) doi:10.1895/wormbook.1.83.2.
35. Zhang, Y., Lu, H. & Bargmann, C. I. Pathogenic bacteria induce aversive olfactory learning in Caenorhabditis elegans. *Nature* **438**, 179–184 (2005).
36. Dirksen, P. *et al.* The native microbiome of the nematode Caenorhabditis elegans: gateway to a new host-microbiome model. *BMC Biol* **14**, 38 (2016).
37. Samuel, B. S., Rowedder, H., Braendle, C., Félix, M.-A. & Ruvkun, G. *Caenorhabditis elegans* responses to bacteria from its natural habitats. *Proceedings of the National Academy of Sciences* **113**, (2016).
38. Berg, M. *et al.* Assembly of the Caenorhabditis elegans gut microbiota from diverse soil microbial environments. *ISME J* **10**, 1998–2009 (2016).
39. Dirksen, P. *et al.* CeMbio - The *Caenorhabditis elegans* Microbiome Resource. *G3 Genes|Genomes|Genetics* **10**, 3025–3039 (2020).

835 40. Yuan, W., Zhou, Y., Fan, Y., Tao, Y. J. & Zhong, W. Orsay δ Protein Is Required for Nonlytic
836 Viral Egress. *J Virol* **92**, (2018).
837 41. Brenner, S. THE GENETICS OF *CAENORHABDITIS ELEGANS*. *Genetics* **77**, 71–94 (1974).
838 42. Troemel, E. R., Félix, M.-A., Whiteman, N. K., Barrière, A. & Ausubel, F. M. Microsporidia
839 Are Natural Intracellular Parasites of the Nematode Caenorhabditis elegans. *PLoS Biol* **6**,
840 e309 (2008).
841 43. Mahajan-Miklos, S., Tan, M.-W., Rahme, L. G. & Ausubel, F. M. Molecular Mechanisms of
842 Bacterial Virulence Elucidated Using a Pseudomonas aeruginosa– Caenorhabditis elegans
843 Pathogenesis Model. *Cell* **96**, 47–56 (1999).
844 44. Rahme, L. G. *et al.* Common Virulence Factors for Bacterial Pathogenicity in Plants and
845 Animals. *Science (1979)* **268**, 1899–1902 (1995).
846 45. Tan, M.-W., Rahme, L. G., Sternberg, J. A., Tompkins, R. G. & Ausubel, F. M. *Pseudomonas*
847 *aeruginosa* killing of *Caenorhabditis elegans* used to identify *P. aeruginosa* virulence
848 factors. *Proceedings of the National Academy of Sciences* **96**, 2408–2413 (1999).
849 46. Kissoyan, K. A. B. *et al.* Exploring Effects of C. elegans Protective Natural Microbiota on
850 Host Physiology. *Front Cell Infect Microbiol* **12**, (2022).
851 47. Jiang, H., Chen, K., Sandoval, L. E., Leung, C. & Wang, D. An Evolutionarily Conserved
852 Pathway Essential for Orsay Virus Infection of *Caenorhabditis elegans*. *mBio* **8**, (2017).
853 48. Lee, J. & Zhang, L. The hierarchy quorum sensing network in Pseudomonas aeruginosa.
854 *Protein Cell* **6**, 26–41 (2015).
855 49. Reimmann, C. *et al.* The global activator GacA of *Pseudomonas aeruginosa* PAO positively
856 controls the production of the autoinducer *N* -butyryl-homoserine lactone and the
857 formation of the virulence factors pyocyanin, cyanide, and lipase. *Mol Microbiol* **24**, 309–
858 319 (1997).
859 50. Parkins, M. D., Ceri, H. & Storey, D. G. Pseudomonas aeruginosa GacA, a factor in
860 multihost virulence, is also essential for biofilm formation. *Mol Microbiol* **40**, 1215–1226
861 (2001).
862 51. Brencic, A. *et al.* The GacS/GacA signal transduction system of *Pseudomonas aeruginosa*
863 acts exclusively through its control over the transcription of the RsmY and RsmZ
864 regulatory small RNAs. *Mol Microbiol* **73**, 434–445 (2009).
865 52. Friedman, L. & Kolter, R. Two Genetic Loci Produce Distinct Carbohydrate-Rich Structural
866 Components of the *Pseudomonas aeruginosa* Biofilm Matrix. *J Bacteriol* **186**, 4457–4465
867 (2004).
868 53. Friedman, L. & Kolter, R. Genes involved in matrix formation in Pseudomonas aeruginosa
869 PA14 biofilms. *Mol Microbiol* **51**, 675–690 (2003).
870 54. Franklin, M. J., Nivens, D. E., Weadge, J. T. & Howell, P. L. Biosynthesis of the
871 Pseudomonas aeruginosa Extracellular Polysaccharides, Alginate, Pel, and Psl. *Front*
872 *Microbiol* **2**, (2011).
873 55. Jackson, K. D., Starkey, M., Kremer, S., Parsek, M. R. & Wozniak, D. J. Identification of *psl* ,
874 a Locus Encoding a Potential Exopolysaccharide That Is Essential for *Pseudomonas*
875 *aeruginosa* PAO1 Biofilm Formation. *J Bacteriol* **186**, 4466–4475 (2004).
876 56. Matsukawa, M. & Greenberg, E. P. Putative Exopolysaccharide Synthesis Genes Influence
877 *Pseudomonas aeruginosa* Biofilm Development. *J Bacteriol* **186**, 4449–4456 (2004).

878 57. Mukherjee, S. *et al.* The PqsE and RhlR proteins are an autoinducer synthase–receptor
879 pair that control virulence and biofilm development in *Pseudomonas aeruginosa*.
880 *Proceedings of the National Academy of Sciences* **115**, (2018).
881 58. Liberati, N. T. *et al.* An ordered, nonredundant library of *Pseudomonas aeruginosa* strain
882 PA14 transposon insertion mutants. *Proceedings of the National Academy of Sciences*
883 **103**, 2833–2838 (2006).
884 59. Simanek, K. A. *et al.* The PqsE-RhlR Interaction Regulates RhlR DNA Binding to Control
885 Virulence Factor Production in *Pseudomonas aeruginosa*. *Microbiol Spectr* **10**, (2022).
886 60. Feinbaum, R. L. *et al.* Genome-Wide Identification of Pseudomonas aeruginosa Virulence-
887 Related Genes Using a Caenorhabditis elegans Infection Model. *PLoS Pathog* **8**, e1002813
888 (2012).
889 61. Xu, L. *et al.* OrthoVenn2: a web server for whole-genome comparison and annotation of
890 orthologous clusters across multiple species. *Nucleic Acids Res* **47**, W52–W58 (2019).
891 62. Sun, J. *et al.* OrthoVenn3: an integrated platform for exploring and visualizing
892 orthologous data across genomes. *Nucleic Acids Res* **51**, W397–W403 (2023).
893 63. McGhee, J. D. The C. elegans intestine. in *WormBook: The Online Review of C. elegans*
894 *Biology* (2007).
895 64. Zhou, Y., Chen, H., Zhong, W. & Tao, Y. J. Collagen and actin network mediate antiviral
896 immunity against Orsay virus in C. elegans intestinal cells. *PLoS Pathog* **20**, e1011366
897 (2024).
898 65. González, R. & Félix, M.-A. Naturally-associated bacteria modulate Orsay virus infection
899 of Caenorhabditis elegans. *PLoS Pathog* **20**, e1011947 (2024).
900 66. Kaul, D. *et al.* Microbiome disturbance and resilience dynamics of the upper respiratory
901 tract during influenza A virus infection. *Nat Commun* **11**, 2537 (2020).
902 67. Lapouge, K., Schubert, M., Allain, F. H.-T. & Haas, D. Gac/Rsm signal transduction
903 pathway of γ-proteobacteria: from RNA recognition to regulation of social behaviour.
904 *Mol Microbiol* **67**, 241–253 (2007).
905 68. Borisovich Shtonda, B. & Avery, L. Dietary choice behavior in Caenorhabditis elegans.
906 doi:10.1242/jeb.01955.
907 69. Hmelo, L. R. *et al.* Precision-engineering the Pseudomonas aeruginosa genome with two-
908 step allelic exchange. *Nat Protoc* **10**, 1820–1841 (2015).
909 70. Rietsch, A., Vallet-Gely, I., Dove, S. L. & Mekalanos, J. J. ExsE, a secreted regulator of type
910 III secretion genes in *Pseudomonas aeruginosa*. *Proceedings of the National Academy of*
911 *Sciences* **102**, 8006–8011 (2005).
912 71. Schneider, C. A., Rasband, W. S. & Eliceiri, K. W. NIH Image to ImageJ: 25 years of image
913 analysis. *Nat Methods* **9**, 671–675 (2012).
914 72. Schindelin, J. *et al.* Fiji: an open-source platform for biological-image analysis. *Nat*
915 *Methods* **9**, 676–682 (2012).
916 73. R Core Team (2022). R: A language and environment for statistical computing. Preprint at
917 (2022).
918 74. Ritz, C., Baty, F., Streibig, J. C. & Gerhard, D. Dose-Response Analysis Using R. *PLOS ONE*
919 **10**, (2015).
920 75. Therneau, T. M. A Package for Survival Analysis in R. Preprint at (2023).

76. Warnes, G. et al. gdata: Various R Programming Tools for Data Manipulation. Preprint at (2022).
77. Wickham H & Seidel D. scales: Scale Functions for Visualization. Preprint at (2022).
78. Hope RM. Rmisc: Ryan Miscellaneous. Preprint at (2022).
79. Hothorn, T., Bretz, F. & Westfall, P. Simultaneous Inference in General Parametric Models. *Biometrical Journal* **50**, 346–363 (2008).
80. Wickham H. *Ggplot2: Elegant Graphics for Data Analysis*. (Springer-Verlag, New York, 2016).
81. Ahlmann-Eltze, C. & Patil, I. ggsignif: R Package for Displaying Significance Brackets for 'ggplot2'. *PsyArxiv* (2021).
82. Wilke C. cowplot: Streamlined Plot Theme and Plot Annotations for 'ggplot2'. Preprint at (2020).

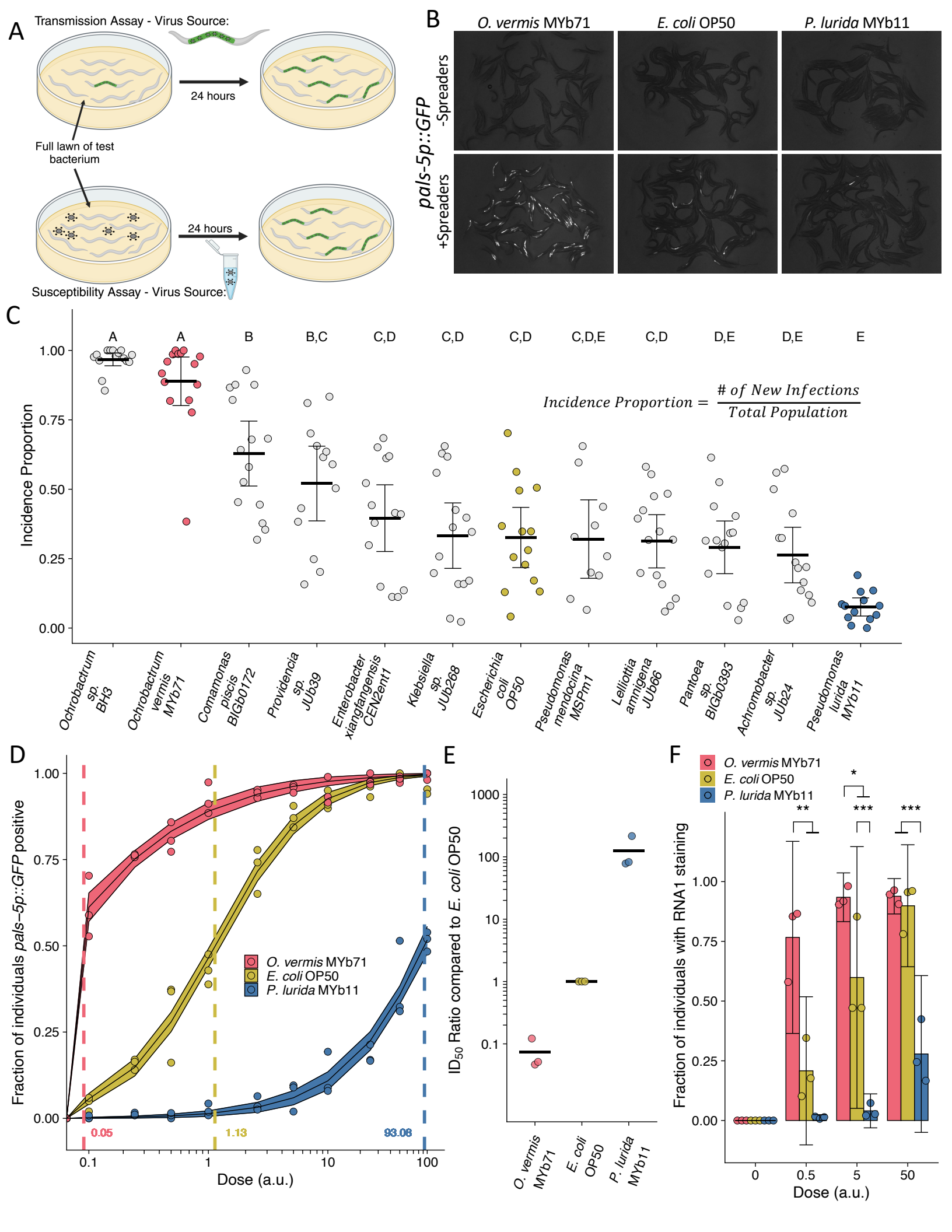
A
Transmission Assay - Virus Source:
24 hours
Full lawn of test bacterium
24 hours
Susceptibility Assay - Virus Source:
B
O. vermis MYb71
E. coli OP50
P. lurida MYb11
pals-5p::GFP
-Spreaders
+Spreaders
C
Incidence Proportion
A A B B,C C,D C,D C,D C,D,E C,D D,E D,E E
Incidence Proportion = # of New Infections / Total Population
Ochrobactrum sp. BH3
Ochrobactrum vermis MYb71
Comamonas piscis BIGb0172
Providencia sp. JUb39
Enterobacter xiangfangensis CEN2ent1
Klebsiella sp. JUb268
Escherichia coli OP50
Pseudomonas mendocina MSPm1
Lelliottia amnigena JUb66
Pantoea sp. BIGb0393
Achromobacter sp. JUb24
Pseudomonas lurida MYb11
D
Fraction of individuals pals-5p::GFP positive
O. vermis MYb71
E. coli OP50
P. lurida MYb11
0.05
1.13
93.08
Dose (a.u.)
E
ID50 Ratio compared to E. coli OP50
O. vermis MYb71
E. coli OP50
P. lurida MYb11
F
O. vermis MYb71
E. coli OP50
P. lurida MYb11
Fraction of individuals with RNA1 staining
Dose (a.u.)

Figure 1: *Ochrobactrum* species and *P. lurida* MYb11 divergently modulate Orsay virus transmission and infection rates.

(A) Schematic representation of the transmission and susceptibility assays: Transmission can be assessed by combining infected spreader individuals (green nematode), uninfected reporter individuals (white nematodes), and various bacteria. Susceptibility can be assessed by combining uninfected reporter individuals with exogenous Orsay virus, and various bacteria. 24 h later, infection is assessed. This schematic was made using Biorender. **(B)** Representative images of *pals-5p::GFP* expression among individuals exposed to spreaders or no spreaders in the presence of *O. vermis* MYb71, *E. coli* OP50, or *P. lurida* MYb11. **(C)** Incidence proportion, calculated as indicated, of Orsay virus transmission quantified on different bacteria from the environment of *C. elegans*. Data shown are from three experiments combined, each dot represents the incidence proportion from a single plate, and letters denote statistical significance. Treatments with the same letter are not significantly different from one another. (n=19694 in total and n > 42 for all dots). **(D)** Dose response curves of *C. elegans* to exogenous Orsay virus. The dashed line indicates the calculated dose at which 50% of the population was infected, the ID_{50}, the exact value which is given above the x-axis for each bacterium. The solid curves represent the 95% confidence interval of the modeled log-logistic function while in the presence of each bacterium. Data are from a single representative experiment and replicates can be found in Supp. Fig. 3, Dots represent individual plates. ((a.u.), arbitrary units, see Methods) (n=8334 in total and n > 32 for all dots). **(E)** Ratios of the ID_{50} calculated on the indicated bacteria as compared to the ID_{50} calculated on *E. coli* OP50 from three separate experiments as in (D) and Supp. Fig. 3. **(F)** The fraction of individuals with staining as assessed by fluorescence *in situ* hybridization targeting the RNA1 segment of Orsay virus. Data shown are from three experiments combined, each dot represents three pooled technical replicate plates from the susceptibility assays in (D) and Supp. Fig. 3. (n=3446 in total and n > 61 for all dots). For all plots the black bar is the mean and error bars are the 95% confidence interval (C.I.). p-values determined using one-way ANOVA followed by Tukey's Honest Significant Difference (HSD) test (NS non-significant, *p<0.05, **p<0.01, ***p<0.001).

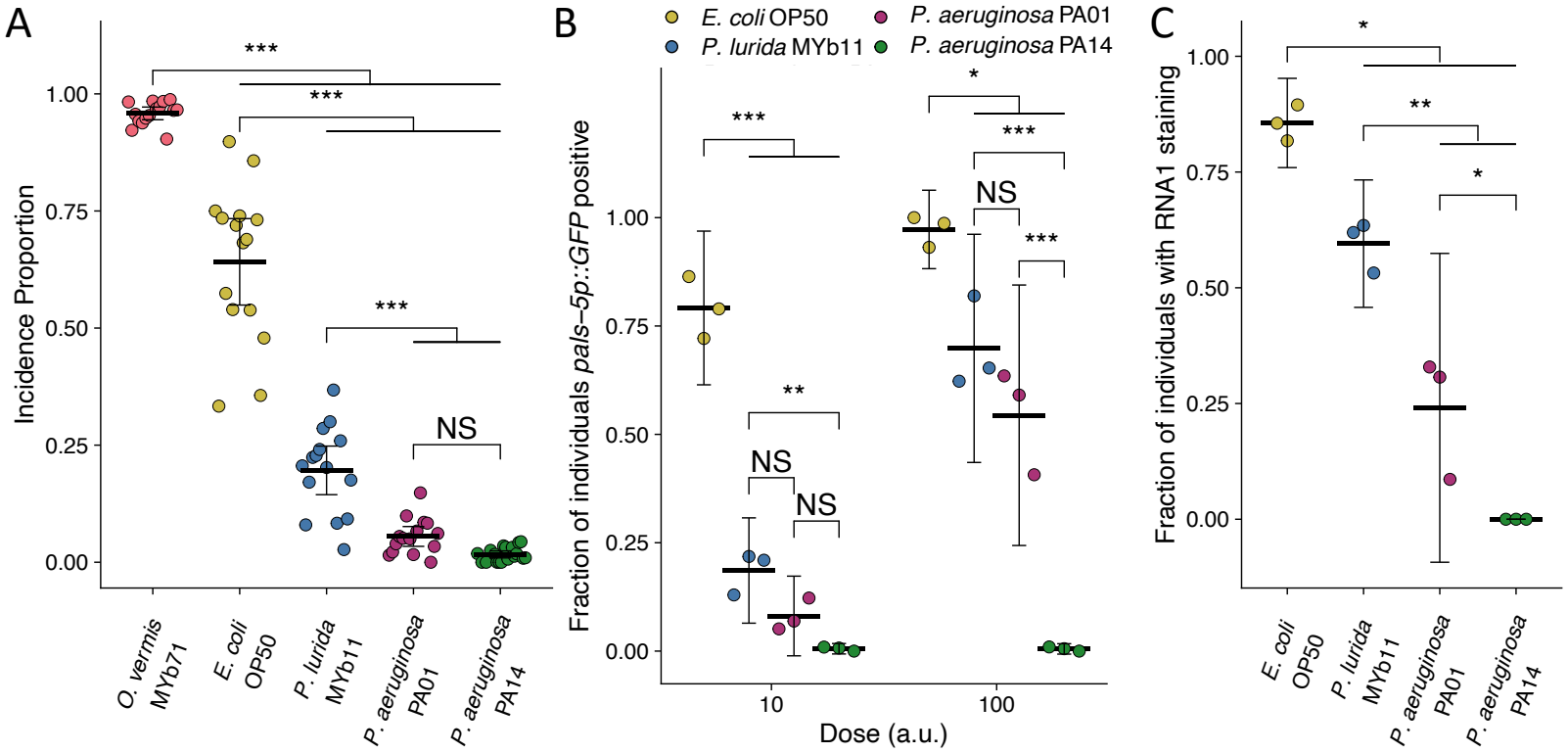
A
Incidence Proportion
1.00
0.75
0.50
0.25
0.00
***
***
***
NS
O. vermis MYb71
E. coli OP50
P. lurida MYb11
P. aeruginosa PA01
P. aeruginosa PA14
B
E. coli OP50
P. lurida MYb11
P. aeruginosa PA01
P. aeruginosa PA14
Fraction of individuals pals–5p::GFP positive
***
**
NS
NS
*
***
NS
***
10
100
Dose (a.u.)
C
Fraction of individuals with RNA1 staining
*
**
*
E. coli OP50
P. lurida MYb11
P. aeruginosa PA01
P. aeruginosa PA14

Figure 2: *P. aeruginosa* attenuates Orsay virus transmission and infection rates.

(A) Incidence proportion of Orsay virus transmission quantified on different bacteria from *C. elegans*' environment and *P. aeruginosa* PA01 and *P. aeruginosa* PA14. Data shown are from three experiments combined, each dot represents the incidence proportion from a single plate. (n=9214 in total and n > 54 for all dots) **(B)** The fraction of individuals *pals-5p::GFP* positive following exposure to two doses of exogenous Orsay virus. Data are from a single representative experiment and replicates can be found in Supp. Fig. 5. Dots represent individual plates. (n=6539 in total and n > 56 for all dots) **(C)** The fraction of individuals with staining following exposure to 100 a.u. Orsay virus as assessed by fluorescence *in situ* hybridization targeting the RNA1 segment of the Orsay virus genome. Data shown are from three experiments combined, each dot represents three pooled technical replicate plates from (B) and Supp. Fig. 5. (n=2743 in total and n > 116 for all dots) For all plots the black bar is the mean and error bars are the 95% confidence interval (C.I.). p-values determined using one-way ANOVA followed by Tukey's Honest Significant Difference (HSD) test (NS non-significant, *p<0.05, **p<0.01, ***p<0.001).

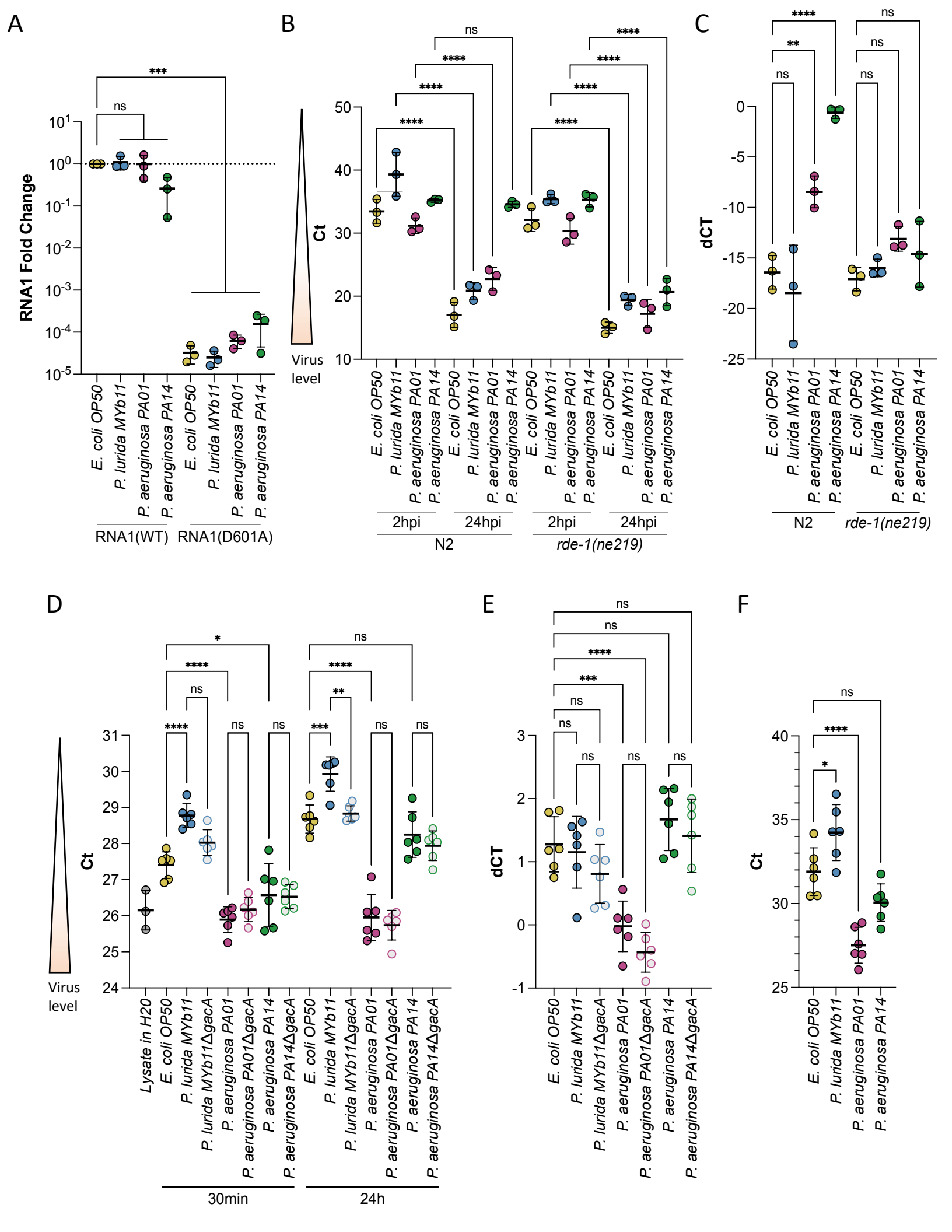
A
RNA1 Fold Change
10^1
10^0
10^{-1}
10^{-2}
10^{-3}
10^{-4}
10^{-5}
***
ns
E. coli OP50
P. lurida MYb11
P. aeruginosa PA01
P. aeruginosa PA14
RNA1(WT)
RNA1(D601A)
B
Virus level
Ct
50
40
30
20
10
****
ns
2hpi
24hpi
N2
rde-1(ne219)
C
dCT
0
-5
-10
-15
-20
-25
****
**
ns
N2
rde-1(ne219)
D
Virus level
Ct
31
30
29
28
27
26
25
24
*
****
ns
***
**
Lysate in H20
E. coli OP50
P. lurida MYb11
P. lurida MYb11ΔgacA
P. aeruginosa PA01
P. aeruginosa PA01ΔgacA
P. aeruginosa PA14
P. aeruginosa PA14ΔgacA
30min
24h
E
dCT
3
2
1
0
-1
****
***
ns
F
Ct
40
35
30
25
****
*
ns

Figure 3: *P. aeruginosa* and *P. lurida* MYb11 do not eliminate Orsay virus replication, rapidly degrade Orsay virus, or eliminate Orsay virus shedding by infected spreader animals.

(A) Animals carrying either a wild-type (RNA1(WT)) or replication defective (RNA1(D601A)) transgenic viral RNA replicon system (Jiang et al. 2017) were used to assess Orsay virus replication efficiency independently of virus entry. P-values determined using one-way ANOVA followed by Dunnett's test **(B)** Orsay virus RNA1 levels of N2 and *rde-1(ne219)* animals exposed to the indicated bacterium and exogenous Orsay virus 2 and 24 h post infection (hpi). P-values were determined using Welch's t-Test For each plot, each dot represents five pooled technical replicates, the black bar is the mean, error bars are the standard deviation, RNA1 levels were quantified by qPCR, and the data shown are for three independent experiments. (**C**) Delta Ct comparing the 24 h and 2 h timepoints from (B). (**D**) Stability of Orsay virus in the presence of lawns of the indicated bacteria for the indicated time at 20°C. (**E**) Delta Ct comparing the 24 h and 30 min timepoints from (D). (**F**) Orsay virus RNA1 levels recovered from the indicated lawns after infected ZD2610(*rde-1(ne219);jyIs8[pals-5p::GFP;myo-2p::mCherry];glp-4(bn2ts)*) spreaders were allowed to shed for 24 hours mimicking a transmission assay. (NS non-significant, *p<0.05, **p<0.01, ***p<0.001).

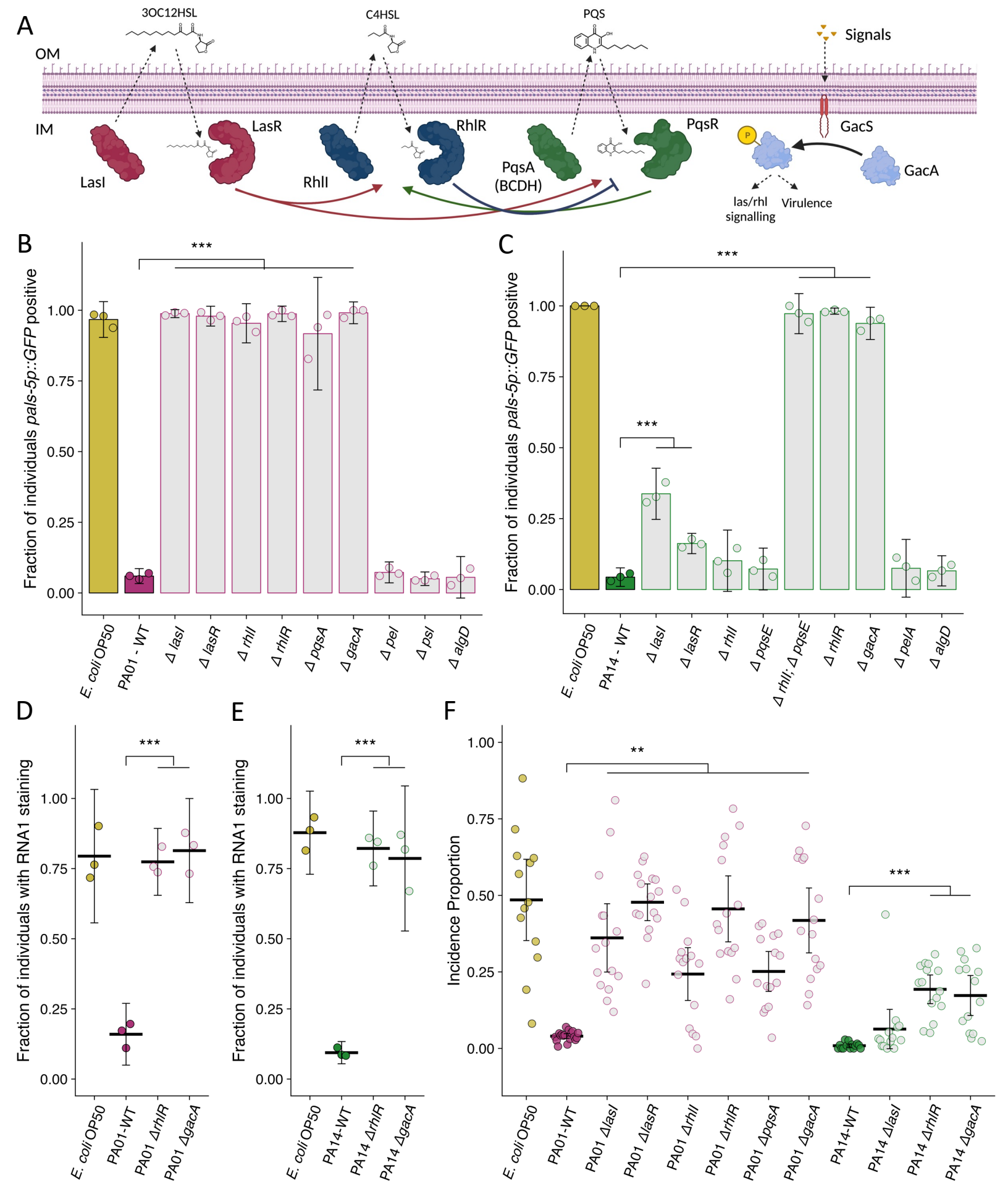
A
3OC12HSL
C4HSL
PQS
Signals
OM
IM
LasR
RhlR
PqsR
GacS
LasI
RhlI
PqsA
(BCDH)
GacA
las/rhl
signalling
Virulence
B
Fraction of individuals pals-5p::GFP positive
E. coli OP50
PA01 - WT
Δ lasI
Δ lasR
Δ rhlI
Δ rhlR
Δ pqsA
Δ gacA
Δ pel
Δ psl
Δ algD
C
Fraction of individuals pals-5p::GFP positive
E. coli OP50
PA14 - WT
Δ lasI
Δ lasR
Δ rhlI
Δ pqsE
Δ rhlI; Δ pqsE
Δ rhlR
Δ gacA
Δ pelA
Δ algD
D
Fraction of individuals with RNA1 staining
E. coli OP50
PA01-WT
PA01 ΔrhlR
PA01 ΔgacA
E
Fraction of individuals with RNA1 staining
E. coli OP50
PA14-WT
PA14 ΔrhlR
PA14 ΔgacA
F
Incidence Proportion
E. coli OP50
PA01-WT
PA01 ΔlasI
PA01 ΔlasR
PA01 ΔrhlI
PA01 ΔrhlR
PA01 ΔpqsA
PA01 ΔgacA
PA14-WT
PA14 ΔlasI
PA14 ΔrhlR
PA14 ΔgacA

Figure 4: Mutation of *P. aeruginosa* quorum sensing regulators and the two-component response regulator *gacA* suppresses the attenuation Orsay virus infection.

(A) Diagram demonstrating the three quorum sensing systems in *P. aeruginosa*. Each system encodes the enzyme(s) (LasI, RhlI, PqsA(BCDH) to produce an autoinducer (3OC12HSL – 3-oxo-C12-homoserine lactone, C4HSL –butanoyl homoserine lactone , PQS – Pseudomonas quinolone signal) that is recognized by its cognate receptor (LasR, RhlR, PqsR) that influences gene transcription and the activity of the other quorum sensing systems. An additional level of regulation stems from the two-component *gacS*/*gacA* system. External signals are recognized by the histidine kinase GacS, which phosphorylates the response regulator GacA that indirectly influences quorum sensing processes. IM is inner membrane, OM is outer membrane. Arrows represent crosstalk between the various system. Adapted from Rutherford and Bassler, 2012 and Song, Li, and Wang, 2023. **(B-C)** The fraction of individuals *pals-5p::GFP* positive following exposure to exogenous Orsay virus in the presence of the indicated bacterium. Data are from a single representative experiment, bars represent mean, dots represent individual plates. **(B)** Wild-type *P. aeruginosa* PA01 compared to mutant *P. aeruginosa* PA01 strains using 10 a.u. of Orsay virus. Replicates can be found in Supp. Fig. 7. (n=4480 in total and n > 76 for all dots) **(C)** Wild-type *P. aeruginosa* PA14 compared to mutant *P. aeruginosa* PA14 strains using 100 a.u. of Orsay virus. Replicates can be found in Supp. Fig. 8. (n=3320 in total and n > 23 for all dots) **(D-E)** The fraction of individuals with staining following exposure to (D) 10 a.u. or (E) 100 a.u. Orsay virus as assessed by fluorescence *in situ* hybridization targeting the RNA1 segment of the Orsay virus genome. Data shown are from three experiments combined, each dot represents three pooled technical replicates from a single experiment. ((D) n=1632 in total and n > 61 for all dots. (E) n=2000 in total and n > 60 for all dots) **(F)** Incidence proportion of Orsay virus transmission in the presence of *P. aeruginosa* wild-type versus select *P. aeruginosa* mutants. Data are from three experiments, bars represent mean, dots represent individual plates. (n=20452 in total and n > 37 for all dots) For all plots error bars represent 95% C.I. For B-E, p-values were determined using one-way ANOVA followed by Dunnett's test. (NS non-significant, *p<0.05, **p<0.01, ***p<0.001).

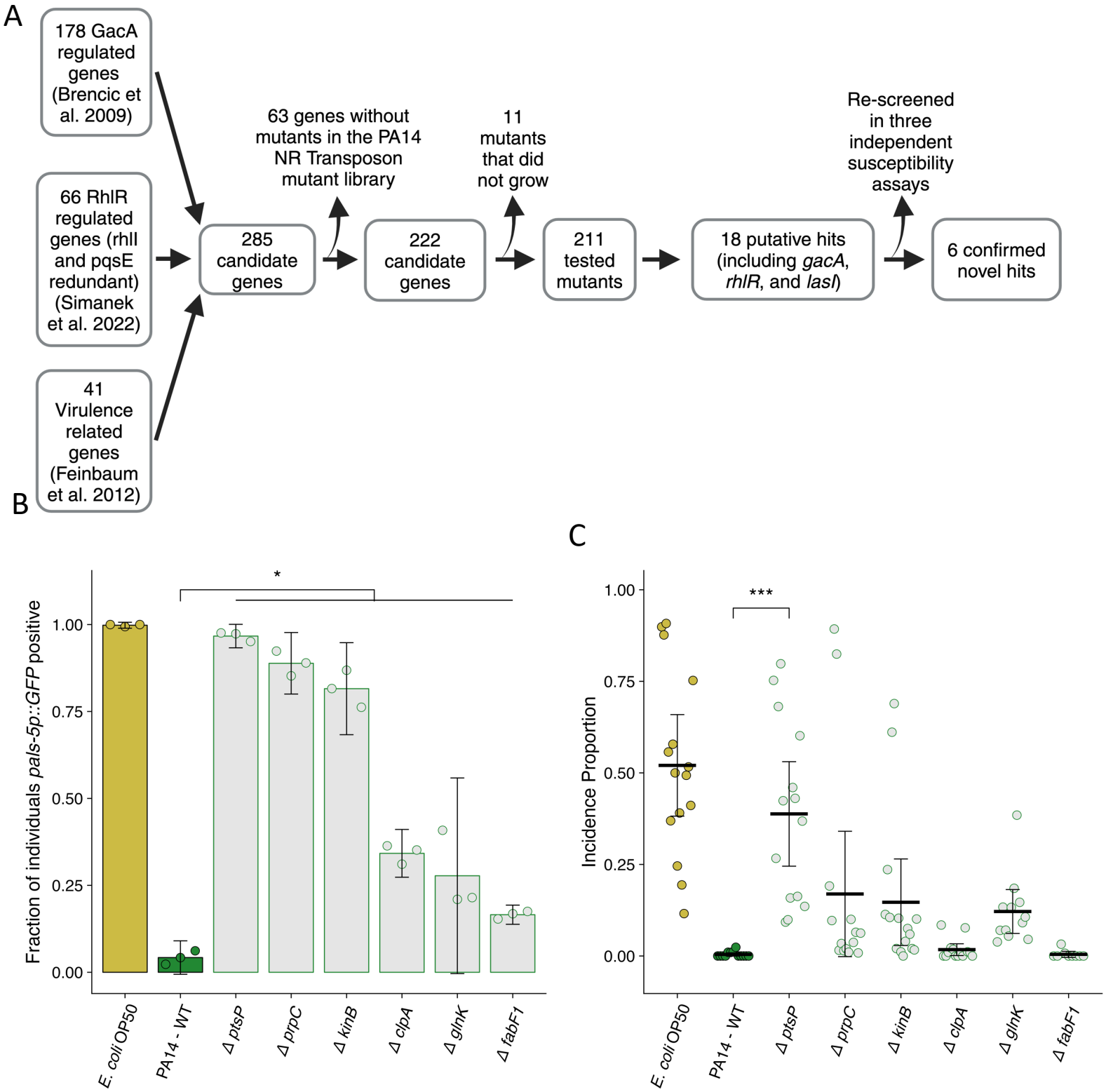
A
178 GacA regulated genes (Brencic et al. 2009)
66 RhlR regulated genes (rhlI and pqsE redundant) (Simanek et al. 2022)
41 Virulence related genes (Feinbaum et al. 2012)
285 candidate genes
63 genes without mutants in the PA14 NR Transposon mutant library
222 candidate genes
11 mutants that did not grow
211 tested mutants
18 putative hits (including gacA, rhlR, and lasI)
Re-screened in three independent susceptibility assays
6 confirmed novel hits
B
Fraction of individuals pals-5p::GFP positive
1.00
0.75
0.50
0.25
0.00
*
E. coli OP50
PA14 - WT
Δ ptsP
Δ prpC
Δ kinB
Δ clpA
Δ glnK
Δ fabF1
C
Incidence Proportion
1.00
0.75
0.50
0.25
0.00
***
E. coli OP50
PA14 - WT
Δ ptsP
Δ prpC
Δ kinB
Δ clpA
Δ glnK
Δ fabF1

Figure 5: Mutation of *P. aeruginosa* PA14 genes related to virulence suppresses the attenuation of Orsay virus infection.

(**A**) Diagram describing the design and results of the screen to identify suppressors of *P. aeruginosa* PA14 Orsay virus attenuation. (**B**) The fraction of individuals *pals-5p::GFP* positive following exposure to 100 a.u. of exogenous Orsay virus. Data are from a single representative experiment. Replicates can be found in Supp. Fig. 10. (n=3779 in total and n > 55 for all dots) (**C**) Incidence proportion of Orsay virus transmission while individuals are present on *P. aeruginosa* PA14 wild-type compared to *P. aeruginosa* PA14 mutants. Data are from three experiments combined and dots represent individual plates. (n=11279 in total and n > 35 for all dots) For all plots the black bar is the mean and error bars are the 95% confidence interval (C.I.). p-values determined using one-way ANOVA followed by Dunnett's test (NS non-significant, *p<0.05, **p<0.01, ***p<0.001).

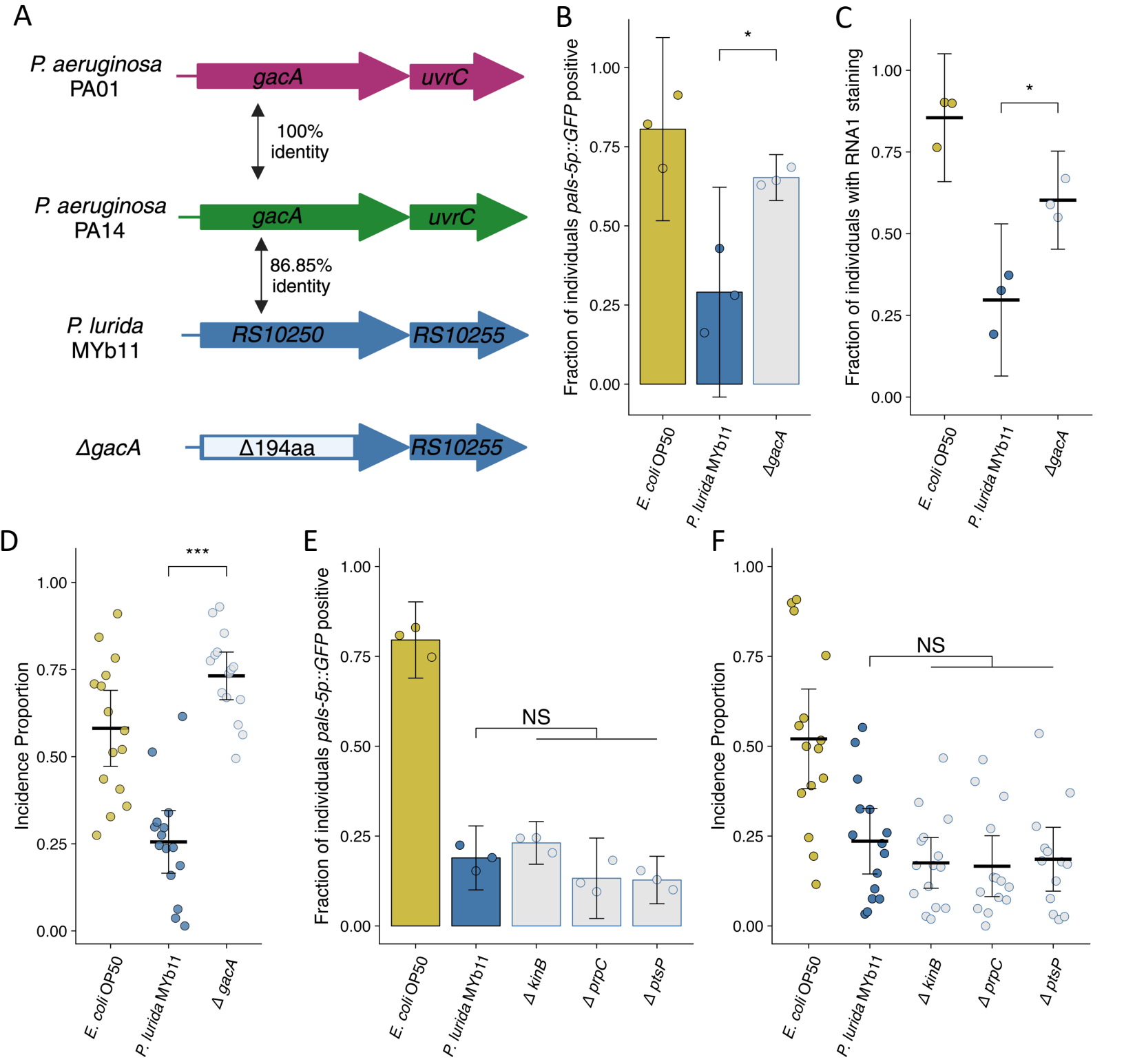
A
P. aeruginosa PA01
gacA
uvrC
100% identity
P. aeruginosa PA14
gacA
uvrC
86.85% identity
P. lurida MYb11
RS10250
RS10255
ΔgacA
Δ194aa
RS10255
B
Fraction of individuals pals-5p::GFP positive
*
E. coli OP50
P. lurida MYb11
ΔgacA
C
Fraction of individuals with RNA1 staining
*
E. coli OP50
P. lurida MYb11
ΔgacA
D
Incidence Proportion
***
E. coli OP50
P. lurida MYb11
Δ gacA
E
Fraction of individuals pals-5p::GFP positive
NS
E. coli OP50
P. lurida MYb11
Δ kinB
Δ prpC
Δ ptsP
F
Incidence Proportion
NS
E. coli OP50
P. lurida MYb11
Δ kinB
Δ prpC
Δ ptsP

Figure 6: Mutation of *P. lurida* MYb11 *gacA* suppresses the attenuation of Orsay virus infection.

(A) Diagram depicting *P. aeruginosa* PA01, *P. aeruginosa* PA14, and *P. lurida* MYb11 *gacA* as well as the *P. lurida* MYb11 *gacA* deletion mutant. Percent identity of the encoded protein was assessed using Clustal Omega. The *gacA* deletion removed 194 amino acids from the protein leaving 10 amino acids from both the N and C termini. Schematic made using Biorender. **(B, E)** The fraction of individuals *pals-5p::GFP* positive following exposure to 10 a.u. exogenous Orsay virus in the presence of wild-type *P. lurida* MYb11 compared to the indicated mutants. Data are from a single representative experiment. Replicates can be found in Supp. Fig. 11. ((B) n=933 in total and n > 46 for all dots, (E) n=1725 in total and n > 78 for all dots). Bars represent mean and dots represent individual plates. **(C)** The fraction of individuals with staining following exposure to 10 a.u. Orsay virus as assessed by fluorescence *in situ* hybridization targeting the RNA1 segment of the Orsay virus genome. Data shown are from three experiments combined, each dot represents three pooled technical replicates from (B) and Supp. Fig 11A and 11B (n=1272 in total and n > 61 for all dots). **(D, F)** Incidence proportion of Orsay virus transmission in the presence of wild-type *P. lurida* MYb11 versus the indicated mutants. Data are from three experiments combined, bars represent mean, dots represent individual plates ((D) n=4534 in total and n > 42 for all dots, (F) n=8185 in total and n > 58 for all dots). For all plots error bars represent 95% confidence interval (C.I.). (B-D) p-values were determined using Student's t-Test. (E-F) p-values determined using one-way ANOVA followed by Dunnett's test (NS non-significant, *p<0.05, **p<0.01, ***p<0.001).

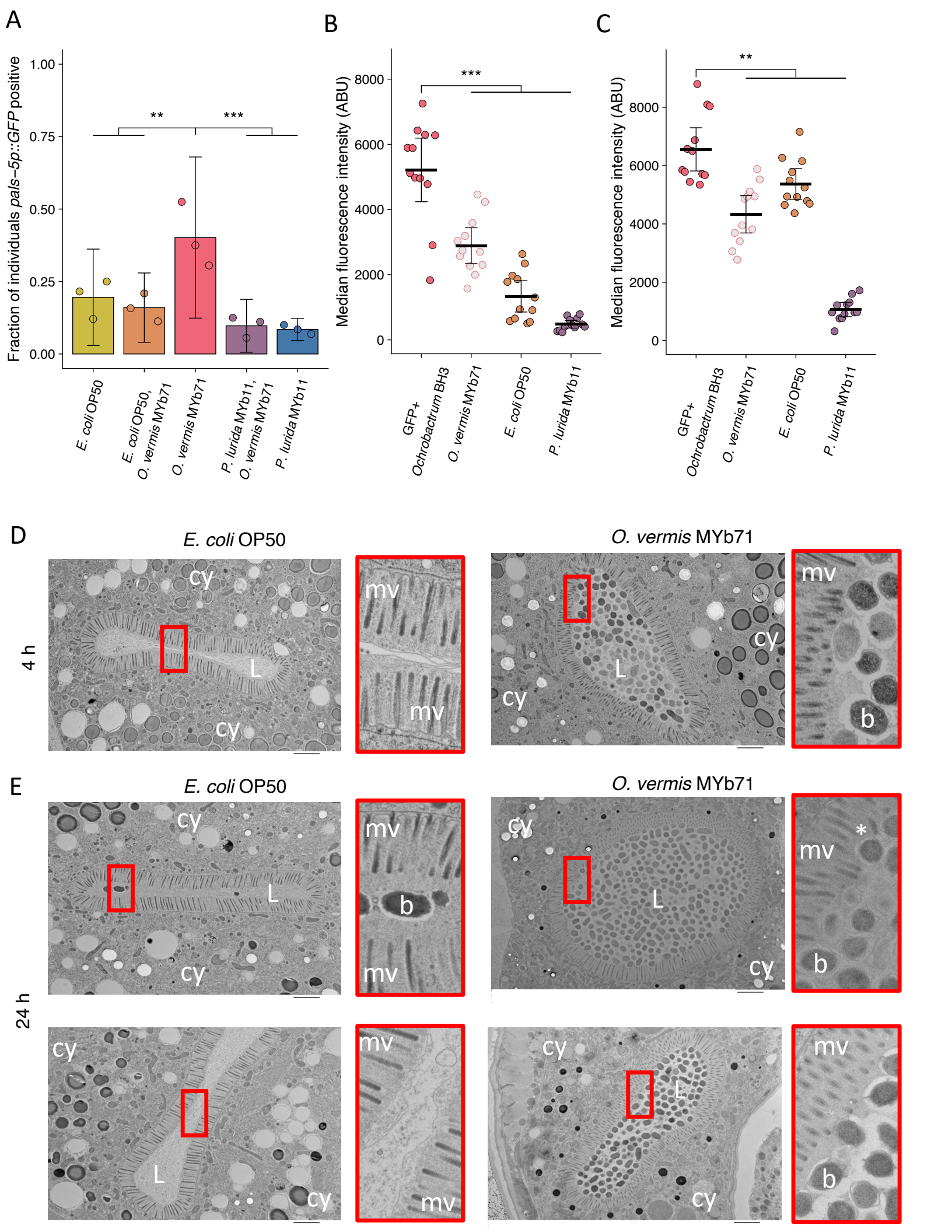
A
Fraction of individuals pals-5p::GFP positive
1.00
0.75
0.50
0.25
0.00
**
***
E. coli OP50
E. coli OP50, O. vermis MYb71
O. vermis MYb71
P. lurida MYb11, O. vermis MYb71
P. lurida MYb11
B
Median fluorescence intensity (ABU)
8000
6000
4000
2000
0
***
GFP+ Ochrobactrum BH3
O. vermis MYb71
E. coli OP50
P. lurida MYb11
C
Median fluorescence intensity (ABU)
8000
6000
4000
2000
0
**
GFP+ Ochrobactrum BH3
O. vermis MYb71
E. coli OP50
P. lurida MYb11
D
E. coli OP50
O. vermis MYb71
4 h
cy
L
mv
b
E
E. coli OP50
O. vermis MYb71
24 h
cy
L
mv
b
*

Figure 7: *O. vermis* MYb71 closely interacts with the brush border of *C. elegans* intestinal cells.

(A) The fraction of individuals *pals-5p::GFP* positive following exposure to 1 a.u. exogenous Orsay virus in the presence of pure lawns of the indicated bacteria or mixed lawns consisting of 50% of the indicated bacteria mixed with 50% *O. vermis* MYb71 (v:v, Methods). Data are from a single representative experiment. Replicates can be found in Supp. Fig. 12. Bars represent mean and dots represent individual plates (n=908 in total and n > 36 for all dots). **(B-C)** The median fluorescence observed in the intestinal lumen of individuals following exposure for (B) 4 h or (C) 24 h to pure GFP expressing *Ochrobactrum* BH3 lawns or mixed lawns consisting of 50% of the indicated bacteria mixed with 50% GFP expressing *Ochrobactrum* BH3 (v:v, Methods). Data are from a single representative experiment. Replicates can be found in Supp. Fig. 12. Bars represent mean, dots represent individual animals. (**D-E**) Electron micrographs of animals exposed to the indicated bacterium for either (D) 4 or (E) 24 h. Scale bar is 2 microns. cy=cytoplasm, L=lumen, mv=microvilli, b=bacterium, and * denotes a bent microvilli. For all plots error bars represent 95% confidence interval (C.I.). p-values determined using one-way ANOVA followed by Dunnett's test (NS non-significant, *p<0.05, **p<0.01, ***p<0.001).

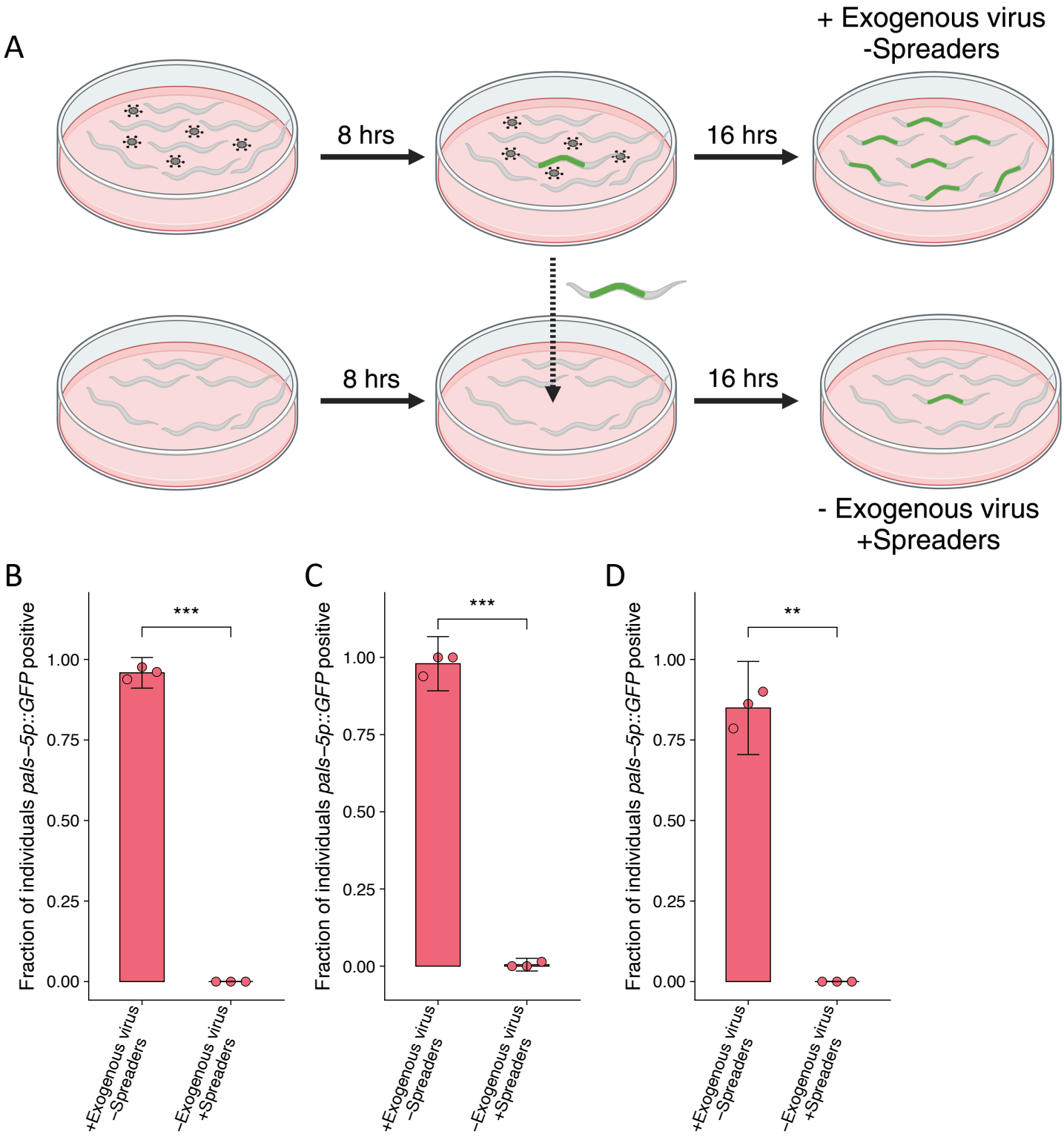

Supplementary Figure 1: Transmission does not occur from individuals infected during the course of a transmission or susceptibility assay.

(A-D) Individuals were exposed to 0 a.u. or 5 a.u. exogenous Orsay virus in the presence of *O. vermis* MYb71. 8 h post infection five infected individuals from the 5 a.u. plate were transferred to the 0 a.u. plate to assess whether transmission from these individuals would occur. Both plates were scored 16 h after the transfer. Data for each plot are from a single representative experiment, bars represent mean, dots represent individual plates ((B) n = 669 in total and n > 83 for all dots, (C) n = 377 in total and n > 52 for all dots, (D) n=273 in total and n > 33 for all dots). Error bars are the 95% confidence interval (C.I.). p-value determined by Student's t-test (NS non-significant, *p<0.05, **p<0.01, ***p<0.001).

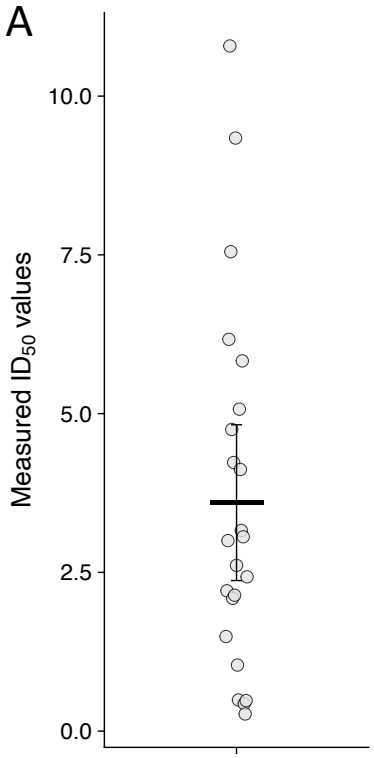

Supplementary Figure 2: The range of all ID_{50} values calculated for each batch of Orsay virus.
(A) Dose response curves as shown in Figure 1D and Supp. Fig. 3 were measured for ZD2611(*jyIs8[pals-5p::GFP; myo-2p::mCherry];glp-4(bn2ts)*) animals exposed to *E. coli* OP50 for each batch of Orsay virus used. The dose of virus required to infect 50% of the population, the ID_{50}, was calculated and plotted. Bar represents the mean and individual dots represent the ID_{50} from a separate dose response curve. Error bars are the 95% confidence interval (C.I.).

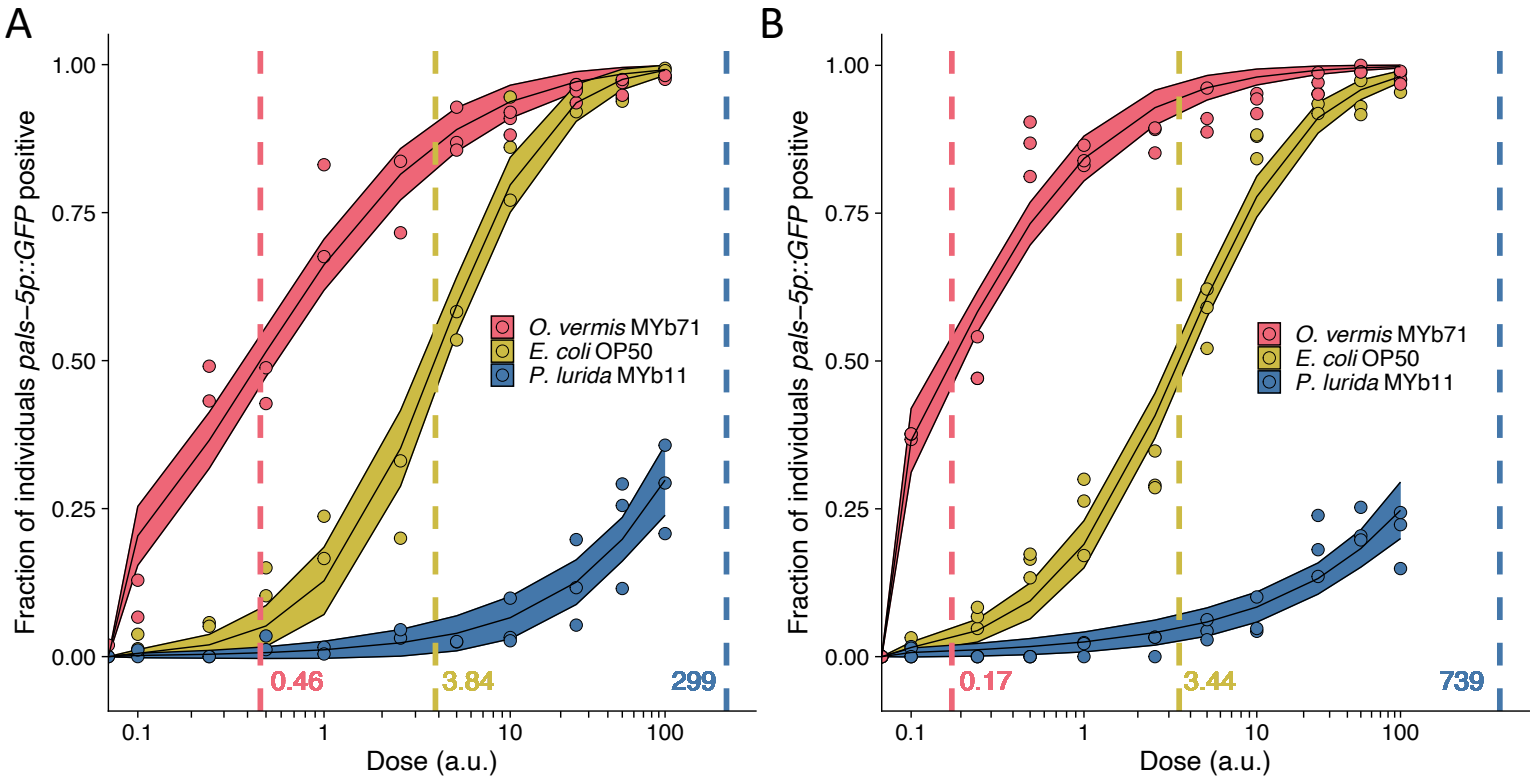

Supplementary Figure 3: Replicate dose response curves shown in Figure 1D.
(A-B) Dose response curves of *C. elegans* to exogenous Orsay virus. The dashed line indicates the calculated dose at which 50% of the population was infected, the ID_{50}, the exact value which is given above the x-axis for each bacterium. The solid curves represent the 95% confidence interval of the modeled log-logistic function while in the presence of each bacterium. Data are from a single representative experiment, Dots represent individual plates((A) n = 11350 in total and n > 38 for all dots, (B) n = 7753 in total and n > 24 for all dots). ((a.u.), arbitrary units).

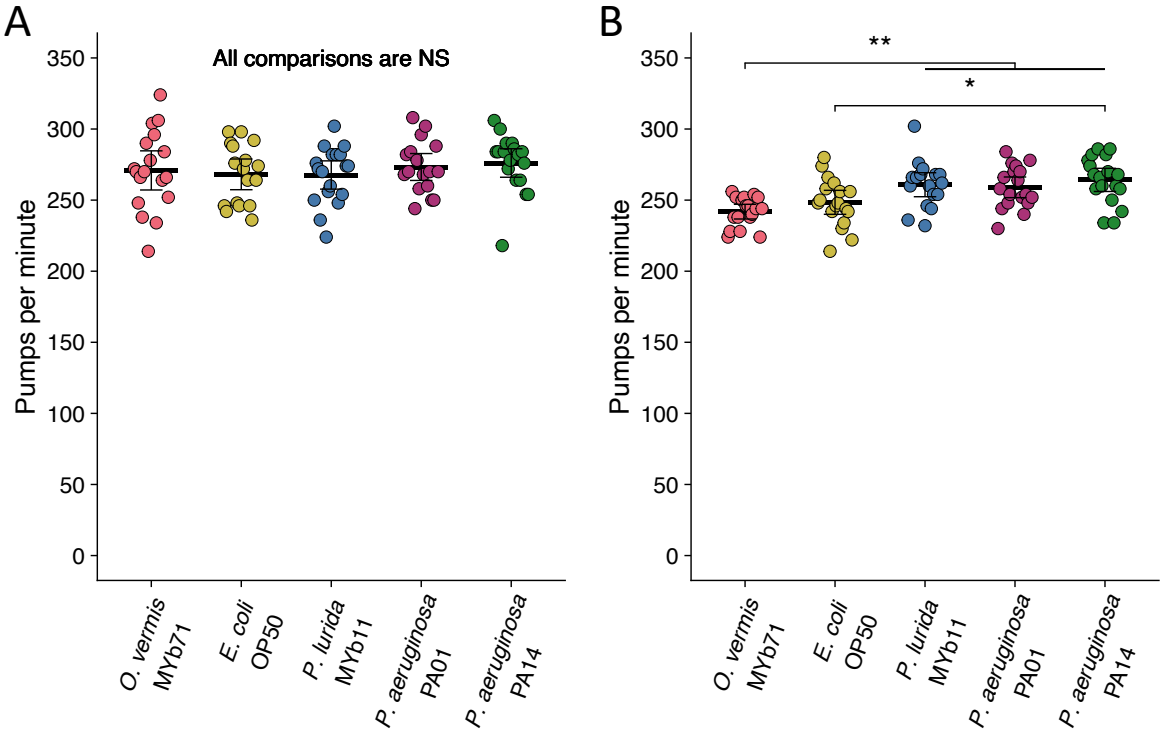

Supplementary Figure 4: Pharyngeal pumping rates are unaltered at 6 h and change only sightly by 24 h after exposure to novel bacteria.

(A-B) Pharyngeal pumping rate of ZD2611 animals exposed to the indicated bacteria for **(A)** 6 or **(B)** 24 h. Pumping rate was assessed via slow-motion video capture of animals feeding (Methods). Data are from three separate experiments and each dot represents a single animal. The black bar is the mean and error bars are the 95% confidence interval (C.I.). p-values determined using one-way ANOVA followed by Tukey's Honest Significant Difference (HSD) test (NS non-significant, *p<0.05, **p<0.01, ***p<0.001).

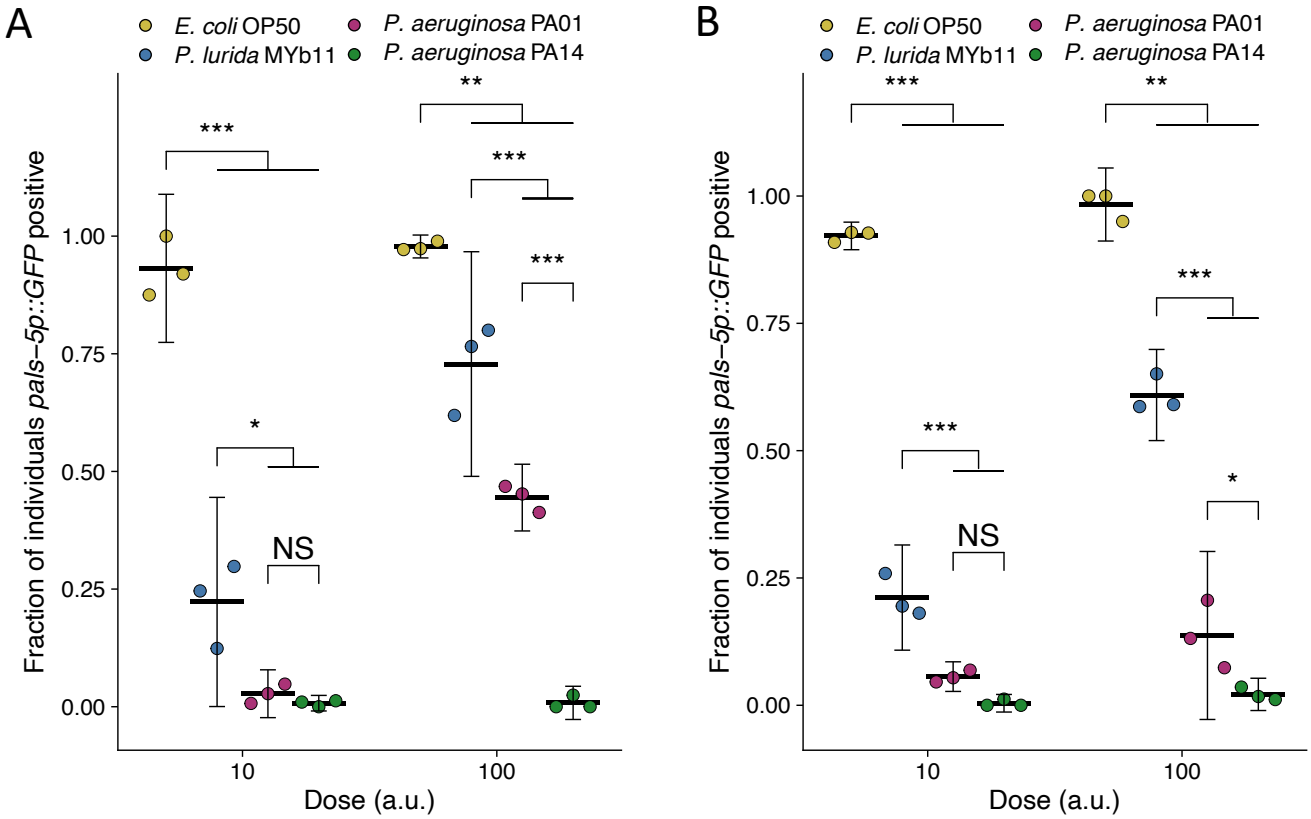

Supplementary Figure 5: Replicate susceptibility assays shown in Figure 2B.
(A-B) The fraction of individuals *pasl-5p::GFP* positive following exposure to two doses of exogenous Orsay virus. Data are from a single representative experiment and dots represent individual plates ((A) n = 2729 total and n > 60 for all dots, ((B) n = 2051 total and n > 48 for all dots). The black bar is the mean and error bars are the 95% confidence interval (C.I.). p-values determined using one-way ANOVA followed by Tukey's Honest Significant Difference (HSD) test (NS non-significant, *p<0.05, **p<0.01, ***p<0.001).

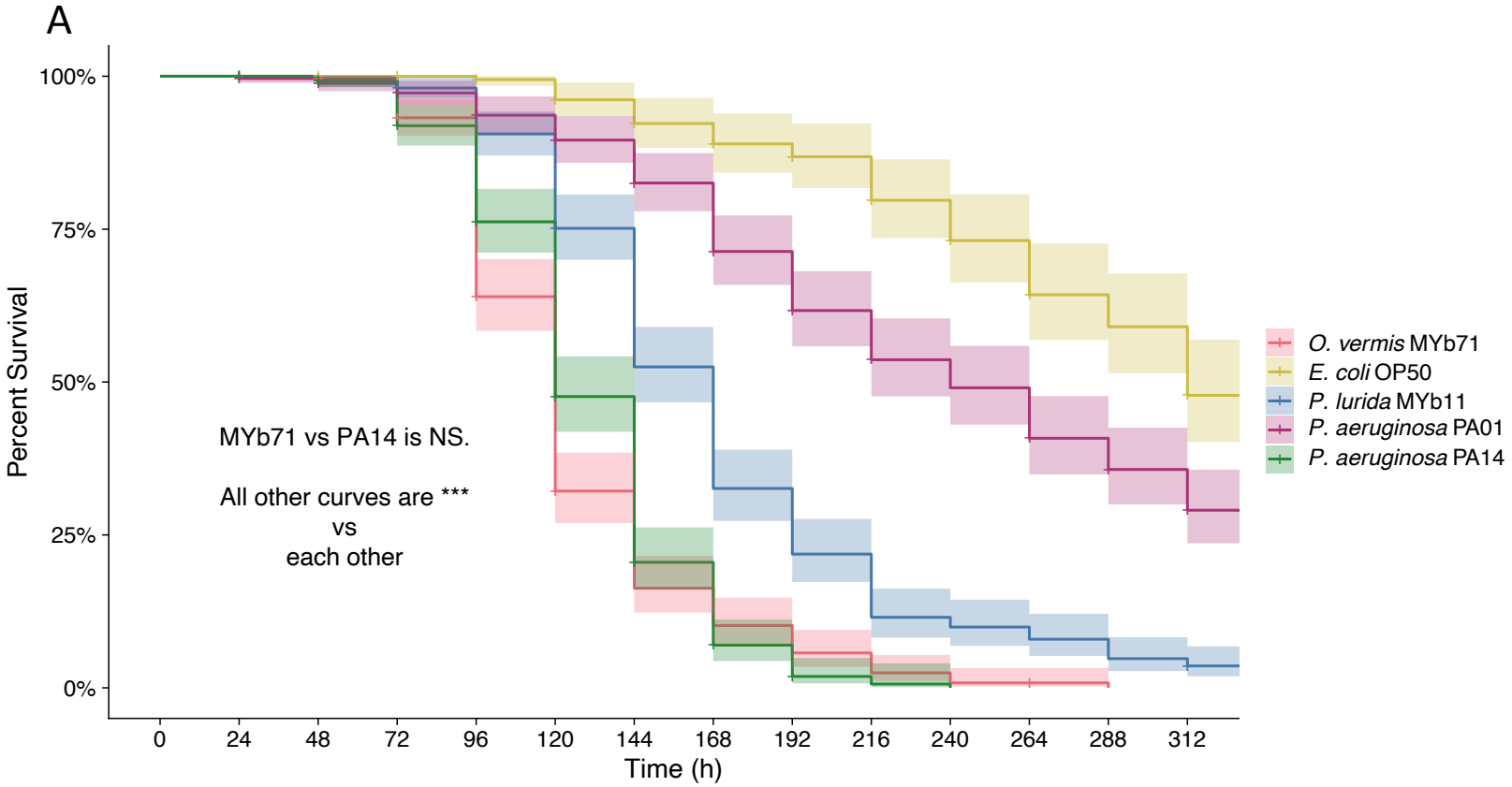

Supplementary Figure 6: *O. vermis* MYb71, *P. aeruginosa* PA14, *P. lurida* MYb11, and *P. aeruginosa* PA01 reduce lifespan compared to *E. coli* OP50 .

(**A**) Survival of ZD2611 animals following exposure to full lawns of the indicated bacteria on fluorodeoxyuridine (FUdR) containing plates at 20°C. Hashes indicate censored animals. Lines represent the Kaplan-Meier curve, while shaded area represents the 95% confidence interval. Curve and confidence interval were calculated from three separate experiments with three replicate plates for each bacteria with approximately 30 individuals per plate. Statistics were calculated with the log-rank test implemented in the survdiff function in the survival package in R followed by the Bonferroni correction. (***p<0.001)

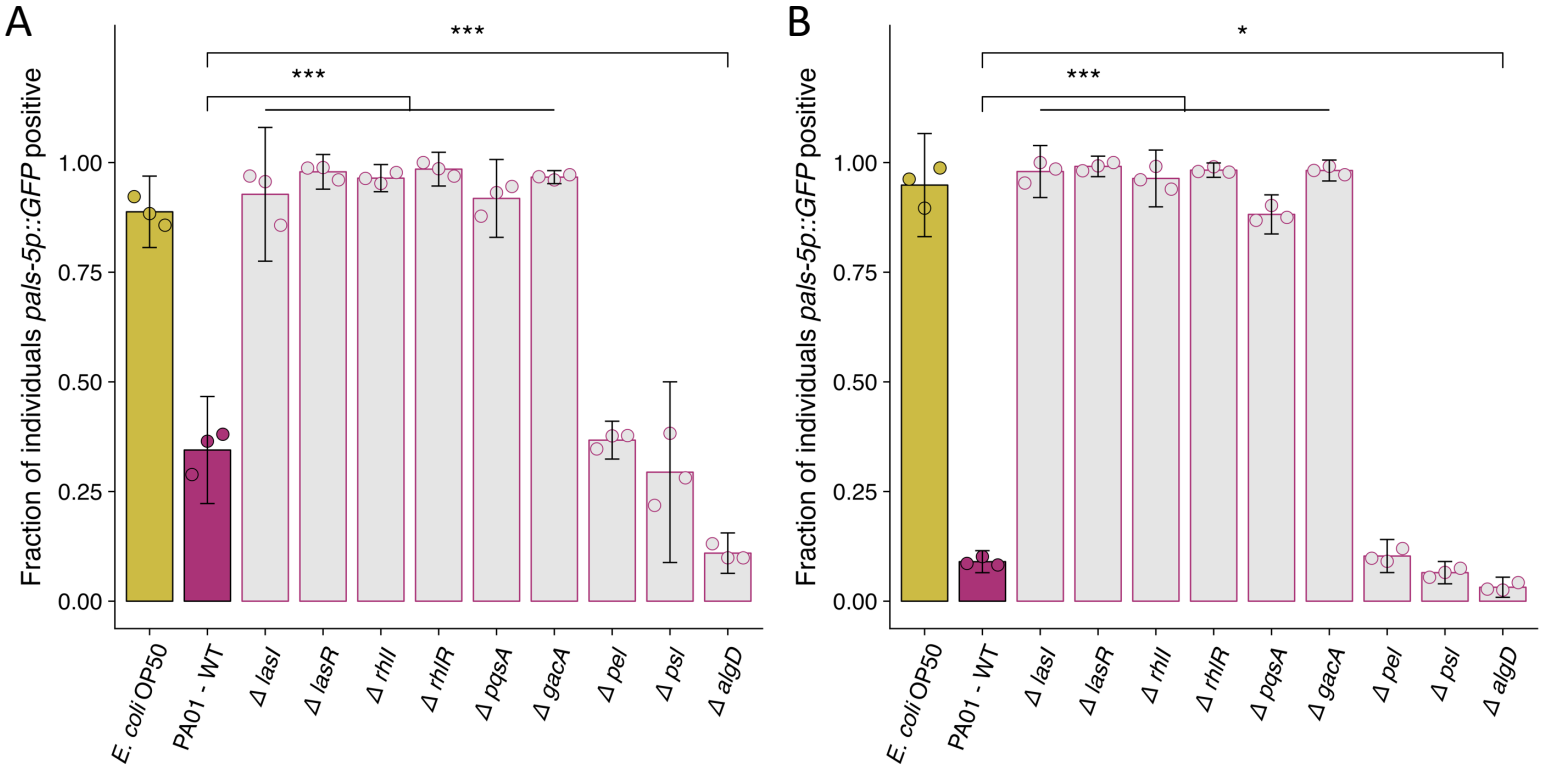

Supplementary Figure 7: Replicate susceptibility assays shown in Figure 4B.
(A-B) The fraction of individuals *pals-5p::GFP* positive following exposure to 10 a.u. of exogenous Orsay virus. Data are from a single representative experiment and dots represent individual plates ((A) n = 2627 in total and n > 43 for all dots, (B) n = 4068 in total and n > 75 for all dots). The black bar is the mean and error bars are the 95% confidence interval (C.I.). p-values determined using one-way ANOVA followed by Dunnett's test (NS non-significant, *p<0.05, **p<0.01, ***p<0.001).

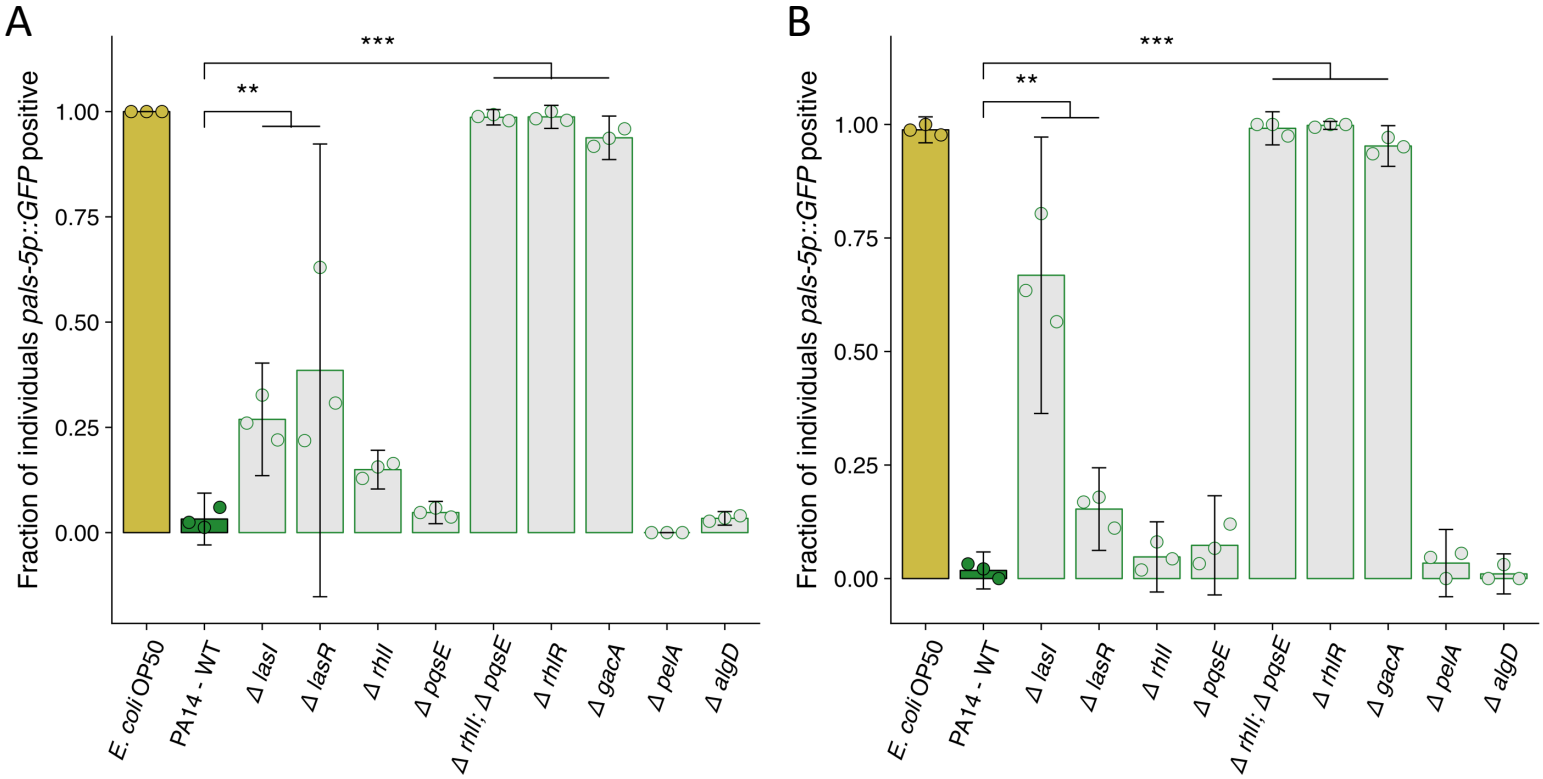

Supplementary Figure 8: Replicate susceptibility assays shown in Figure 4C.
(A-B) The fraction of individuals *pals-5p::GFP* positive following exposure to 100 a.u. of exogenous Orsay virus. Data are from a single representative experiment and dots represent individual plates ((A) n = 3672 in total and n > 37 for all dots, (B) n = 2728 in total and n > 23 for all dots). The black bar is the mean and error bars are the 95% confidence interval (C.I.). p-values determined using one-way ANOVA followed by Dunnett's test (NS non-significant, *p<0.05, **p<0.01, ***p<0.001).

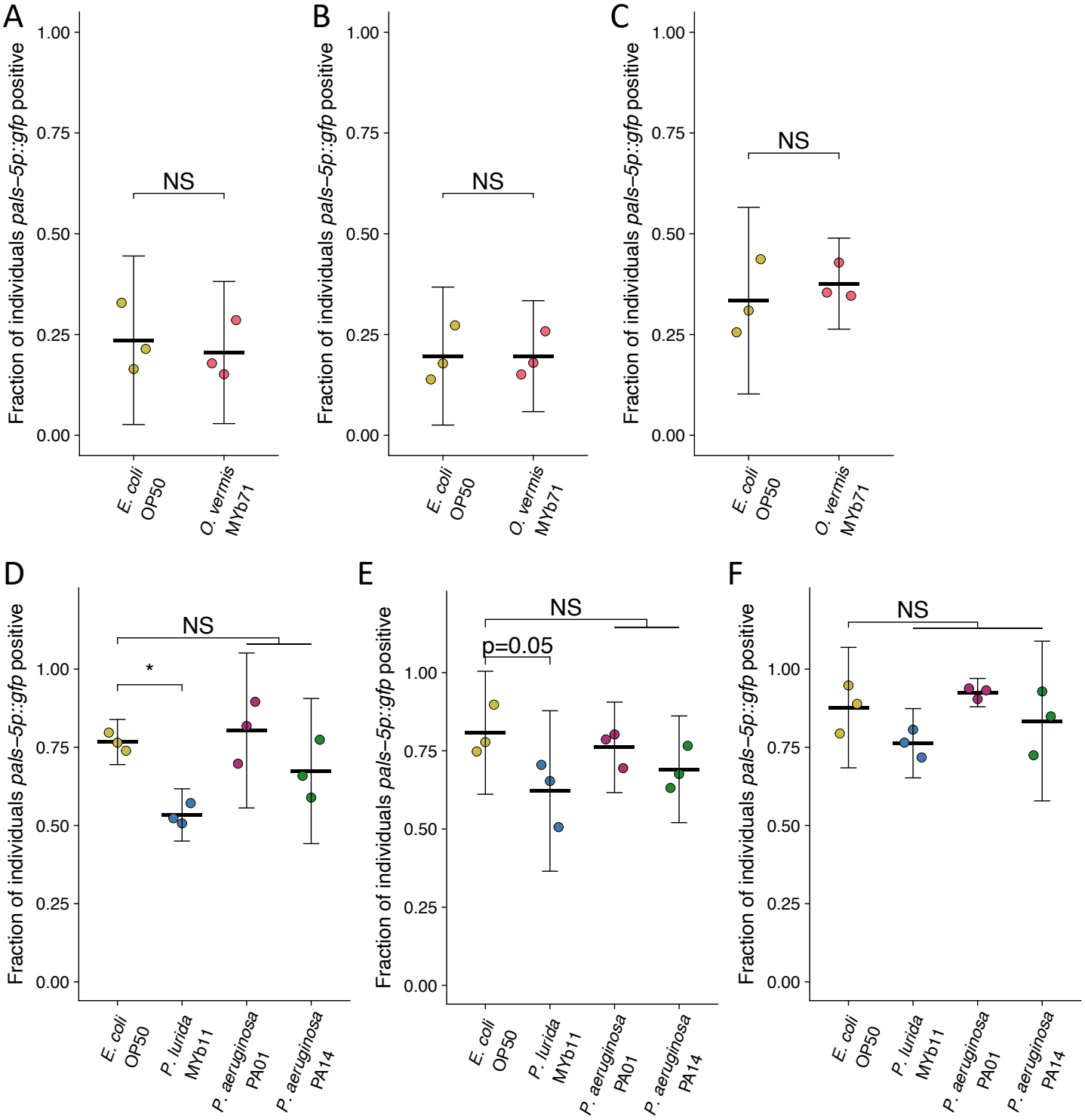

Supplementary Figure 9: Supernatant from stationary phase cultures of different bacteria does not reliably attenuate or enhance Orsay virus infection in the presence of *E. coli* OP50.
(A-F) The fraction of individuals GFP positive following exposure to (A-C) 0.5 a.u. or (D-F) 5 a.u. of exogenous Orsay virus in the presence of *E. coli* OP50 saturated stationary phase supernatant from the indicated bacteria. Data from each plot are from a single experiment. The black bar is the mean, error bars are the 95% confidence interval (C.I.), and dots represent individual plates ((A) n = 384 in total and n > 35 for all dots, (B) n = 525 in total and n > 55 for all dots, (C) n = 881 in total and n > 103 for all dots, (D) n = 843 in total and n > 46 for all dots, (E) n = 1040 in total and n > 39 for all dots, (F) n = 1603 in total and n > 86 for all dots). (A-C) p-values determined using Student's t-test. (D-E) p-values determined using a one-way ANOVA followed by Dunnett's test (NS non-significant, *p<0.05, **p<0.01, ***p<0.001).

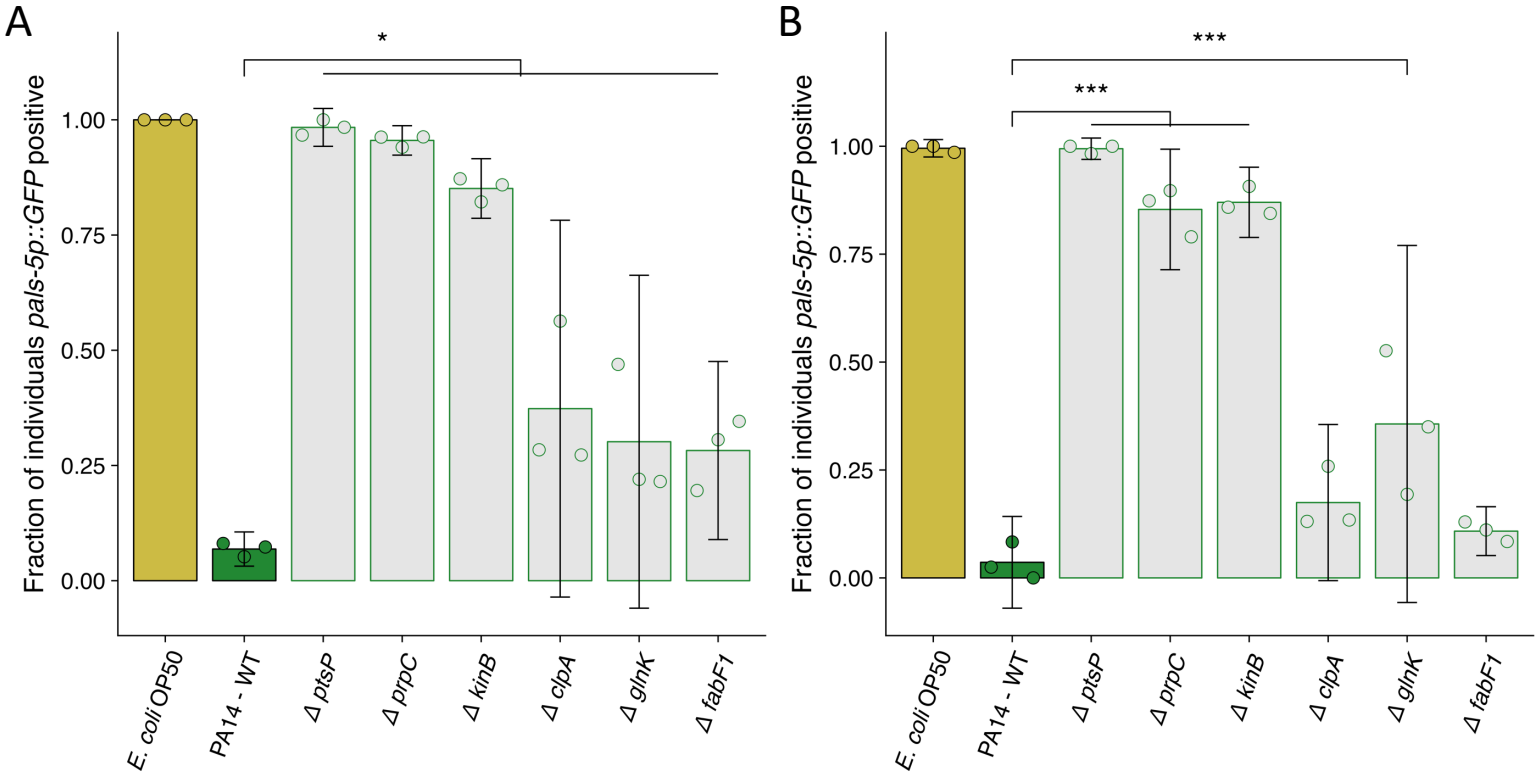

Supplementary Figure 10: Replicate susceptibility assays shown in Figure 5B.
(A-B) The fraction of individuals *pals-5p::GFP* positive following exposure to 100 a.u. of exogenous Orsay virus. Data are from a single representative experiment and dots represent individual plates ((A) n = 1957 in total and n > 33 for all dots, (B) n = 1730 in total and n > 24 for all dots). The black bar is the mean and error bars are the 95% confidence interval (C.I.). p-values determined using one-way ANOVA followed by Dunnett's test (NS non-significant, *p<0.05, **p<0.01, ***p<0.001).

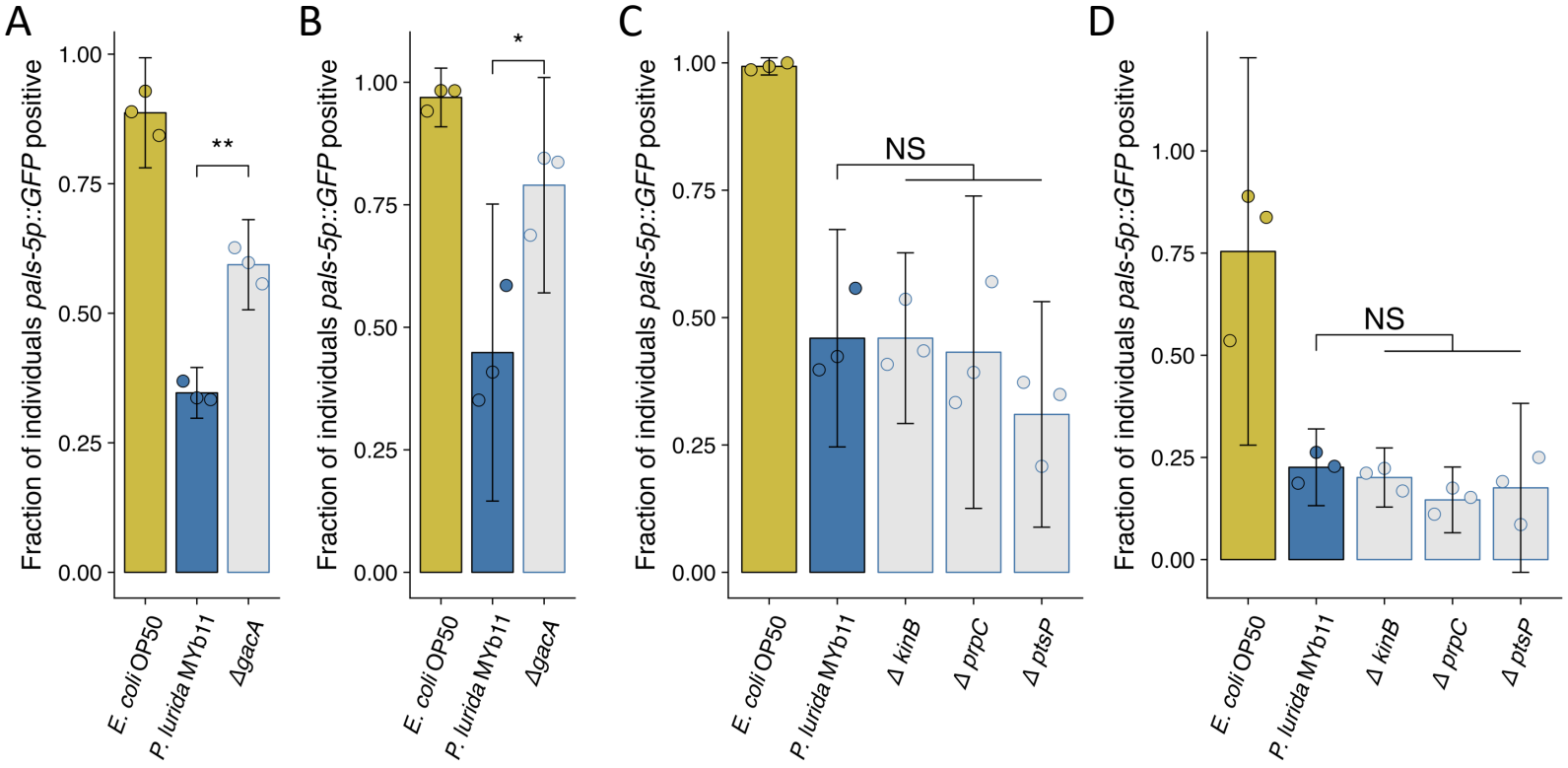

Supplementary Figure 11: Replicate susceptibility assays shown in Figure 6B and 6E.
(A-D) The fraction of individuals *pals-5p::GFP* positive following exposure to 10 a.u. exogenous Orsay virus in the presence of wild-type *P. lurida* MYb11 versus the indicated mutants. Data are from a single representative experiment and dots represent individual plates ((A) n = 681 in total and n > 39 for all dots, (B) n = 751 in total and n > 41 for all dots, (C) n = 2129 in total and n > 106 for all dots, (D) n = 1466 in total and n > 28 for all dots). For all plots the bar is the mean and error bars are the 95% confidence interval (C.I.). A-B) p-values determined using Student's t-test. (C-D) p-values determined using one-way ANOVA followed by Dunnett's test(NS non-significant, *p<0.05, **p<0.01, ***p<0.001).

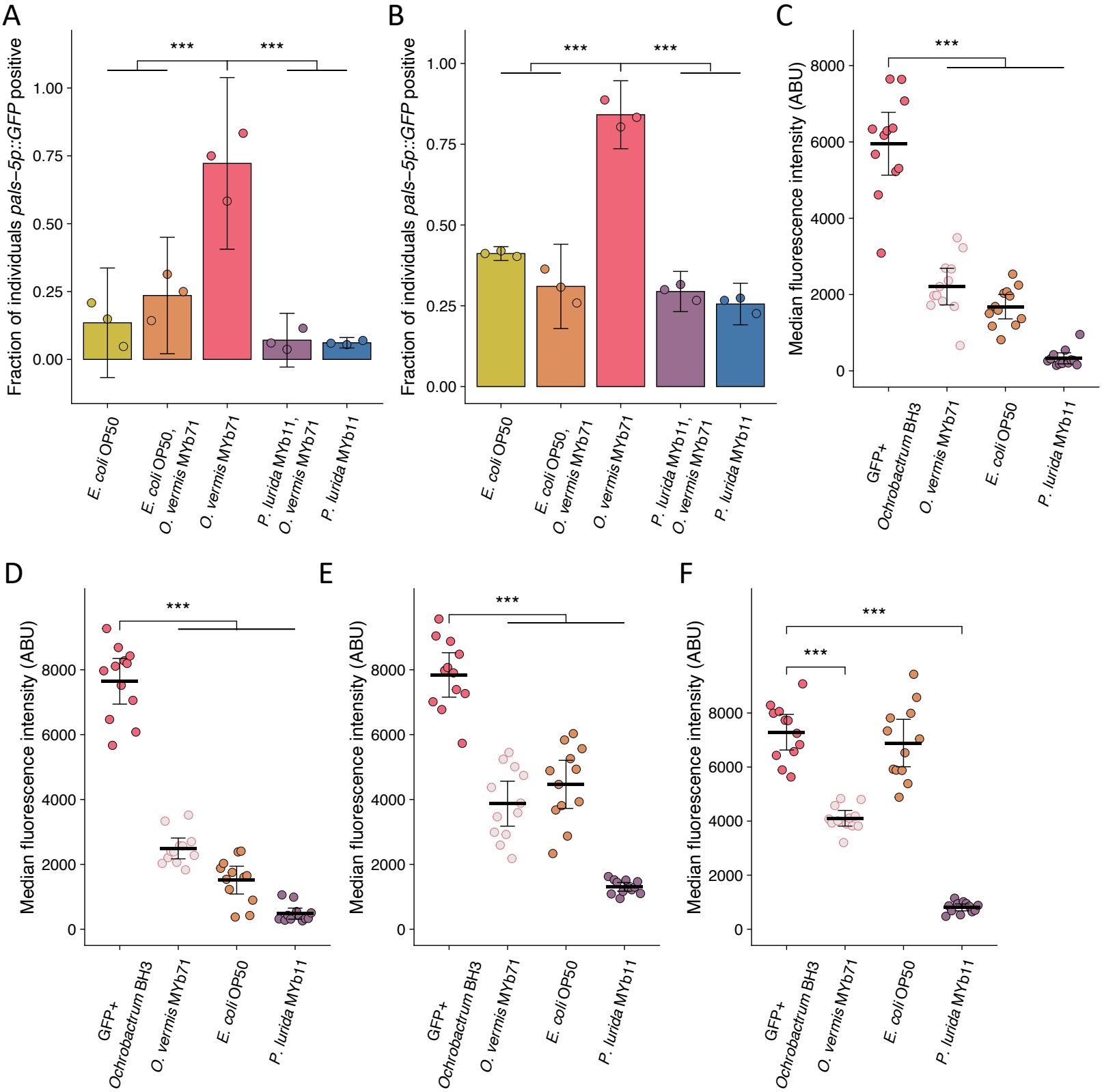

Supplementary Figure 12: Replicate assays shown in Figure 7A, 7B, and 7C.
(A-B) The fraction of individuals *pals-5p::GFP* positive following exposure to 1 a.u. exogenous Orsay virus in the presence of pure lawns of the indicated bacteria or mixed lawns consisting of 50% of the indicated bacteria mixed with 50% *O. vermis* MYb71 (v:v, Methods). Data are from a single representative experiment. Bars represent mean and dots represent individual plates ((A) n=886 in total and n > 43 for all dots, (B) n=833 in total and n > 30 for all dots). **(C-F)** The median fluorescence observed in the intestinal lumen of individuals following exposure for (C-D) 4 h or (E-F) 24 h to pure GFP expressing *Ochrobactrum* BH3 lawns or mixed lawns consisting of 50% of the indicated bacteria mixed with 50% GFP expressing *Ochrobactrum* BH3 (v:v, Methods). Data are from a single representative experiment. Bars represent mean, dots represent individual animals. For all plots error bars represent 95% confidence interval (C.I.). p-values determined using one-way ANOVA followed by Dunnett's test (NS non-significant, *p<0.05, **p<0.01, ***p<0.001).

Supplementary Information

Supplementary Table 1: List of *Caenorhabditis elegans* strains used in this study.

Strain Name	Genotype	Source
WUM29	*virIs1[pHIP::Orsay-RNA1;pHIP::Orsay-RNA2;myo-2p::YFP];rde-1(ne219);jyIs8(pasl-5p::gfp;myo-2p::mCherry)*	Gift of Wang lab[1]
ERT54	*jyIs8[pals-5p::GFP;myo-2p::mCherry]*	CGC
WUM31	*rde-1(ne219);jyIs8[pals-5p::GFP;myo-2p::mCherry]*	Gift of Wang lab[2]
SS104	*glp-4(bn-2)*	CGC
ZD2610	*rde-1(ne219);jyIs8[pals-5p::GFP;myo-2p::mCherry]; glp-4(bn-2)*	This study
ZD2611	*jyIs8[pals-5p::GFP;myo-2p::mCherry]; glp-4(bn-2)*	This study
WUM104	*virEx[pHIP::RNA1WT-1]*	Gift of Wang lab[2]
WUM106	*virEx[pHIP::RNA1D601A-1]*	Gift of Wang lab[2]

Supplementary Table 2: List of bacterial strains used in this study.

Strain Name	Genotype	Source
Escherichia coli OP50	WT	Kim Lab
Enterobacter xiangfangensis CEN2ent1	WT	CGC[3]
Lelliottia amnigena JUb66	WT	CGC[3]
Pseudomonas mendocina MSPm1	WT	CGC[3]
Comamonas piscis BIGb0172	WT	CGC[3]
Pantoea sp. BIGb0393	WT	CGC[3]
Providencia sp. JUb39	WT	Gift of Félix Lab[4]
Klebsiella sp. JUb268	WT	Gift of Félix Lab – unpublished
Achromobacter sp. JUb24	WT	Gift of Félix Lab[4]
Ochrobactrum vermis MYb71	WT	CGC[3]
Ochrobactrum BH3	WT	Gift of Troemel Lab[5]
GFP + Ochrobactrum BH3	WT(GFP+)	Gift of Troemel Lab[5]
Pseudomonas lurida MYb11	WT	CGC[3]
Pseudomonas lurida MYb11	ΔgacA	This study
Pseudomonas lurida MYb11	ΔkinB	This study
Pseudomonas lurida MYb11	ΔprpC	This study
Pseudomonas lurida MYb11	ΔptsP	This study
Pseudomonas aeruginosa PA01	WT	Gift of Dove Lab
Pseudomonas aeruginosa PA01	ΔlasI	Gift of Greenberg Lab[6]
Pseudomonas aeruginosa PA01	ΔlasR	Gift of Greenberg Lab[6]
Pseudomonas aeruginosa PA01	ΔrhlI	Gift of Greenberg Lab[6]
Pseudomonas aeruginosa PA01	ΔrhlR	Gift of Greenberg Lab[6]
Pseudomonas aeruginosa PA01	ΔpqsA	Gift of Dove Lab - unpublished
Pseudomonas aeruginosa PA01	ΔgacA	Gift of Dove Lab[7]
Pseudomonas aeruginosa PA01	Δpel	Gift of Parsek Lab[8]
Pseudomonas aeruginosa PA01	Δpsl	Gift of Parsek Lab[9]
Pseudomonas aeruginosa PA01	ΔalgD	Gift of Parsek Lab[10]
Pseudomonas aeruginosa PA14	WT	Kim Lab
Pseudomonas aeruginosa PA14	ΔlasI	Gift of E. Drenkard and Ausubel Lab – Not published
Pseudomonas aeruginosa PA14	ΔlasR	Gift of E. Drenkard and Ausubel Lab[11]
Pseudomonas aeruginosa PA14	ΔrhlI	Gift of E. Drenkard and Ausubel Lab[12]
Pseudomonas aeruginosa PA14	ΔrhlR	Gift of E. Drenkard and Ausubel Lab[11]
Pseudomonas aeruginosa PA14	ΔpqsE	Gift of Paczkowski Lab[13]
Pseudomonas aeruginosa PA14	ΔrhlI;ΔpqsE	Gift of Paczkowski Lab[13]
Pseudomonas aeruginosa PA14	ΔgacA	Gift of Pukkila-Worley Lab[14]
Pseudomonas aeruginosa PA14	ΔpelA	Gift of E. Drenkard and Ausubel Lab[15]
Pseudomonas aeruginosa PA14	ΔalgD	Gift of E. Drenkard and Ausubel Lab[16]

Pseudomonas aeruginosa PA14	Mutants from the Nonredundant PA14 Transposon Insertion Library	E. Drenkard and Ausubel Lab[14]

Supplementary Table 3: List of *P. aeruginosa* PA14 transposon insertion mutants screened in this study.

Bold and underlined indicate mutants with confirmed phenotype.

Identifier	Identifier	Regulon	Mutant ID
PA14_39800	fecI	gacA	5297
PA14_63160	pmrB	gacA	5751
PA14_19020	tse3	gacA	6047
PA14_43900		Virulence	6472
PA14_55170	cat	gacA	6692
PA14_42340	pscD	gacA	6764
PA14_06750	nitrite reductase;protein_id=QDL62541.1	RhlR	6811
PA14_09660		gacA	23248
PA14_43050	PA01-tssA1	gacA	23266
PA14_42470	pcrV	gacA	23320
PA14_19100	alpha/beta hydrolase;protein_id=QDL63509.1	RhlR	23291
PA14_12030		Virulence	23465
PA14_23430		Virulence	23782
PA14_09300		Virulence	23790
PA14_09300		gacA	23790
PA14_52690		Virulence	24118
PA14_46680	norM	gacA	24085
PA14_06720	protein nirF;protein_id=QDL62538.1	RhlR	24165
PA14_15080		gacA	24311
PA14_26230	hisQ	gacA	24643
PA14_28130	bswR	gacA	24728
PA14_21000	hypothetical protein;protein_id=QDL63663.1	RhlR	25384
PA14_21000	hypothetical protein;protein_id=QDL63663.1	RhlR	25384
PA14_15200		gacA	25712
PA14_42950		Virulence	25708
PA14_36290	NADP-dependent oxidoreductase;protein_id=QDL64899.1	RhlR	25752
PA14_06180	fecI	gacA	25794
PA14_58030	fumC1	gacA	25811
PA14_40310	acyl carrier protein;protein_id=QDL65222.1	RhlR	26047
PA14_39440		gacA	26130
PA14_39790		gacA	26678
PA14_42620	pscR	gacA	26713
PA14_70720		gacA	26837
PA14_52230	pirA	gacA	27108
PA14_14850		Virulence	27116
PA14_37260	OprD family porin;protein_id=QDL64986.1	RhlR	27286
PA14_55580	hemO	gacA	27752
PA14_53910	No clear ortholog	gacA	27823
PA14_48520	transglycosylase;protein_id=QDL65879.1	RhlR	27859
PA14_36310	cyanide-forming glycine dehydrogenase subunit HcnC;protein_id=QDL64901.1	RhlR	28000
PA14_21680		gacA	28071
PA14_07330		gacA	28734
PA14_10200	fvbA	gacA	28811
PA14_31370	methyltransferase domain-containing protein;protein_id=QDL64513.1	RhlR	28925
PA14_01150	eagt6	gacA	28943
PA14_09690	bfiS	gacA	28988
PA14_38950		gacA	29098
PA14_21020	non-ribosomal peptide synthetase;protein_id=QDL63665.1	RhlR	29306
PA14_09630		gacA	29508

PA14_56090		gacA	29512
PA14_42350	pscC	gacA	29579
PA14_20960	nuclear transport factor 2 family protein;protein_id=QDL63660.1	RhlR	29854
PA14_04340		gacA	29941
PA14_3885	exaB	gacA	30227
PA14_60650		gacA	30214
PA14_01140	tse6	gacA	30560
PA14_64920	methyl-accepting chemotaxis protein;protein_id=QDL67201.1	RhlR	30889
PA14_65170	rpsR	gacA	31176
PA14_58570		gacA	31335
PA14_52670		Virulence	31424
PA14_29650	psl and pyoverdine operon regulator PpyR;protein_id=QDL64369.1	RhlR	31563
PA14_43350		Virulence	31640
PA14_02910	IclR family transcriptional regulator;protein_id=QDL62237.1	RhlR	31642
PA14_42400	exsB	gacA	31713
PA14_47380	hxuA	gacA	31886
PA14_00890	pppA	gacA	31907
PA14_52660		Virulence	32331
PA14_58040		gacA	32484
PA14_23000	carbohydrate ABC transporter permease;protein_id=QDL63835.1	RhlR	32514
PA14_58250	magD	gacA	32575
PA14_27700		Virulence	32578
PA14_14340		gacA	33029
PA14_28895		gacA	33357
PA14_63770	Also hits PA14_63760	gacA	33569
PA14_31730		gacA	33612
PA14_31350	NAD(P)/FAD-dependent oxidoreductase;protein_id=QDL67941.1	RhlR	33671
PA14_69810	**glnK**	**Virulence**	**33817**
PA14_34130	icmF3	gacA	34003
PA14_25690	**fabF1**	**Virulence**	**34095**
PA14_33260	pvdS	gacA	34241
PA14_22990		gacA	34541
PA14_42450	popB	gacA	34677
PA14_42440	popD	gacA	34677
PA14_30650	**gacA**	**Virulence**	**34781**
PA14_31580		Virulence	34827
PA14_34050	hsiC3	gacA	34884
PA14_58010		gacA	34966
PA14_71100	YeiH family protein;protein_id=QDL67678.1	RhlR	35049
PA14_71840		gacA	35192
PA14_36300	TetR/AcrR family transcriptional regulator;protein_id=QDL64900.1	RhlR	35194
PA14_40290	protease LasA;protein_id=QDL65220.1	RhlR	35267
PA14_28350	alpha/beta hydrolase;protein_id=QDL64257.1	RhlR	35370
PA14_09350		gacA	35518
PA14_72390	**kinB**	**Virulence**	**35639**
PA14_09320		Virulence	35711
PA14_38770	pqqH	gacA	35762
PA14_23460		Virulence	35855
PA14_52130	wzz2	gacA	35858
PA14_05960		Virulence	36116
PA14_20580	aliphatic amidase expression-regulating protein;protein_id=QDL63629.1	RhlR	36129
PA14_04410	**ptsP**	**Virulence**	**36275**
PA14_58000	sodM	gacA	36454
PA14_63220		gacA	36489

PA14_37250	MFS transporter;protein_id=QDL64985.1	RhlR	36598
PA14_38820	pqqB	gacA	36607
PA14_01030	hcp1	gacA	36995
PA14_01030	hcp3	gacA	36995
PA14_00560	exoT	gacA	36955
PA14_07360		gacA	36956
PA14_00080		gacA	37111
PA14_11660	aqpZ	gacA	37239
PA14_00580		gacA	37604
PA14_54640		Virulence	37629
PA14_16160		gacA	37763
PA14_69000		Virulence	37818
PA14_19120	**RhlR**	**Virulence**	**37943**
PA14_38900	eraR	gacA	38131
PA14_14330	spcS	gacA	38258
PA14_49750	MFS transporter;protein_id=QDL65983.1	RhlR	38758
PA14_20970	cytochrome P450;protein_id=QDL63661.1	RhlR	38837
PA14_38440		Virulence	38983
PA14_53940		Virulence	39064
PA14_45940		Virulence	39292
PA14_30230	**clpA**	**Virulence**	**39351**
PA14_11120	response regulator transcription factor;protein_id=QDL62884.1	RhlR	39369
PA14_62280	hmuV	gacA	39440
PA14_00820	tagQ1	gacA	39485
PA14_39000		gacA	39587
PA14_02140	siaB	gacA	39659
PA14_38190		gacA	39754
PA14_20190	nitrous oxide reductase family maturation protein NosD;protein_id=QDL63598.1	RhlR	39889
PA14_34110	dotU3	gacA	40266
PA14_52580		Virulence	40436
PA14_35130	ArsR family transcriptional regulator;protein_id=QDL64805.1	RhlR	40419
PA14_53950	**prpC**	**Virulence**	**41035**
PA14_38840	exaC	gacA	41052
PA14_32880		gacA	41110
PA14_42430	exsC	gacA	41125
PA14_28000		gacA	41577
PA14_38200		gacA	41886
PA14_22980	carbohydrate ABC transporter substrate-binding protein;protein_id=QDL63833.1	RhlR	42223
PA14_36330	hcnA	gacA	42284
PA14_01010	hsiB1	gacA	42268
PA14_01010	hsiB2	gacA	42268
PA14_01010	hsiB3	gacA	42268
PA14_63120	spermidine synthase;protein_id=QDL68019.1	RhlR	42429
PA14_63120	speE2	gacA	42429
PA14_38780	pqqE	gacA	42390
PA14_00940	tssK1	gacA	42462
PA14_67530		gacA	42570
PA14_68730		Virulence	42600
PA14_05310		Virulence	42799
PA14_16180		gacA	42990
PA14_56890	mexW	gacA	43547
PA14_63800	mgtA	gacA	43710
PA14_31720		gacA	43724
PA14_15990	trmD	gacA	43735

PA14_29660	short-chain dehydrogenase;protein_id=QDL64370.1	RhlR	43837
PA14_21030	ATP-dependent Clp protease proteolytic subunit;protein_id=QDL63666.1	RhlR	44009
PA14_63130		gacA	44414
PA14_20200	nitrous-oxide reductase;protein_id=QDL63599.1	RhlR	44533
PA14_18860	No clear ortholog	gacA	44571
PA14_42270	pscJ	gacA	45034
PA14_38220		gacA	45228
PA14_09970	fpvB	gacA	45188
PA14_51380		Virulence	45262
PA14_47110		gacA	45355
PA14_38860	exaA	gacA	45932
PA14_61190	cdrB	gacA	45954
PA14_51250		gacA	46490
PA14_24990		gacA	46692
PA14_62810	secG	gacA	47247
PA14_48590		Virulence	47923
PA14_49740	hypothetical protein;protein_id=QDL67981.1	RhlR	48441
PA14_49740		gacA	48441
PA14_01020	hsiC2	gacA	48448
PA14_63580	fdnH	gacA	48501
PA14_42460	pcrH	gacA	48586
PA14_62290	phuU	gacA	48599
PA14_08360	trpC	gacA	48714
PA14_20230	regulatory protein NosR;protein_id=QDL63600.1	RhlR	48720
PA14_08370		Virulence	52692
PA14_42380	exsD	gacA	52698
PA14_30580		Virulence	52787
PA14_57990		gacA	52805
PA14_22020		Virulence	52889
PA14_62350	phuR	gacA	53271
PA14_41710		Virulence	53876
PA14_36350		gacA	54275
PA14_40030		gacA	54445
PA14_52840		gacA	54510
PA14_64940	nicotinate-nicotinamide nucleotide adenylyltransferase;protein_id=QDL67203.1	RhlR	54555
PA14_16270		gacA	54625
PA14_53640		gacA	54847
PA14_20020	hasAp	gacA	55211
PA14_33050		gacA	55625
PA14_39990		gacA	55689
PA14_02110	siaD	gacA	55715
PA14_41730		Virulence	55833
PA14_20920	class I SAM-dependent methyltransferase;protein_id=QDL63657.1	RhlR	55954
PA14_38800	pqqC	gacA	56080
PA14_01120	tsi6	gacA	56172
PA14_01100	clpV1	gacA	56461
PA14_52720		Virulence	56790
PA14_72050		gacA	57004
PA14_52260		Virulence	42741
PA14_61680		Virulence	46240
PA14_38970	ercS'	gacA	1242
PA14_31700		gacA	738
PA14_42280	pscI	gacA	383

Supplementary References

1. Jiang, H., Franz, C. J. & Wang, D. Engineering Recombinant Orsay Virus Directly in the Metazoan Host Caenorhabditis elegans. *J Virol* **88**, 11774–11781 (2014).
2. Jiang, H., Chen, K., Sandoval, L. E., Leung, C. & Wang, D. An Evolutionarily Conserved Pathway Essential for Orsay Virus Infection of *Caenorhabditis elegans*. *mBio* **8**, (2017).
3. Dirksen, P. *et al.* CeMbio - The *Caenorhabditis elegans* Microbiome Resource. *G3 Genes|Genomes|Genetics* **10**, 3025–3039 (2020).
4. Samuel, B. S., Rowedder, H., Braendle, C., Félix, M.-A. & Ruvkun, G. *Caenorhabditis elegans* responses to bacteria from its natural habitats. *Proceedings of the National Academy of Sciences* **113**, (2016).
5. Troemel, E. R., Félix, M.-A., Whiteman, N. K., Barrière, A. & Ausubel, F. M. Microsporidia Are Natural Intracellular Parasites of the Nematode Caenorhabditis elegans. *PLoS Biol* **6**, e309 (2008).
6. Wang, M., Schaefer, A. L., Dandekar, A. A. & Greenberg, E. P. Quorum sensing and policing of *Pseudomonas aeruginosa* social cheaters. *Proceedings of the National Academy of Sciences* **112**, 2187–2191 (2015).
7. Brencic, A. *et al.* The GacS/GacA signal transduction system of *Pseudomonas aeruginosa* acts exclusively through its control over the transcription of the RsmY and RsmZ regulatory small RNAs. *Mol Microbiol* **73**, 434–445 (2009).
8. Starkey, M. *et al. Pseudomonas aeruginosa* Rugose Small-Colony Variants Have Adaptations That Likely Promote Persistence in the Cystic Fibrosis Lung. *J Bacteriol* **191**, 3492–3503 (2009).
9. Kirisits, M. J., Prost, L., Starkey, M. & Parsek, M. R. Characterization of Colony Morphology Variants Isolated from *Pseudomonas aeruginosa* Biofilms. *Appl Environ Microbiol* **71**, 4809–4821 (2005).
10. Wozniak, D. J. *et al.* Alginate is not a significant component of the extracellular polysaccharide matrix of PA14 and PAO1 *Pseudomonas aeruginosa* biofilms. *Proceedings of the National Academy of Sciences* **100**, 7907–7912 (2003).
11. Limmer, S. *et al. Pseudomonas aeruginosa* RhlR is required to neutralize the cellular immune response in a *Drosophila melanogaster* oral infection model. *Proceedings of the National Academy of Sciences* **108**, 17378–17383 (2011).
12. Haller, S. *et al.* Quorum-sensing regulator RhlR but not its autoinducer RhlI enables *Pseudomonas* to evade opsonization. *EMBO Rep* **19**, (2018).
13. Simanek, K. A. *et al.* The PqsE-RhlR Interaction Regulates RhlR DNA Binding to Control Virulence Factor Production in *Pseudomonas aeruginosa*. *Microbiol Spectr* **10**, (2022).
14. Liberati, N. T. *et al.* An ordered, nonredundant library of *Pseudomonas aeruginosa* strain PA14 transposon insertion mutants. *Proceedings of the National Academy of Sciences* **103**, 2833–2838 (2006).
15. Friedman, L. & Kolter, R. Genes involved in matrix formation in Pseudomonas aeruginosa PA14 biofilms. *Mol Microbiol* **51**, 675–690 (2003).

16. Yorgey, P., Rahme, L. G., Tan, M. W. & Ausubel, F. M. The roles of mucD and alginate in the virulence of Pseudomonas aeruginosa in plants, nematodes and mice. *Mol Microbiol* **41**, 1063–76 (2001).